Inorganic Chemistry

Article

pubs.acs.org/IC

# Optimization of the Sensitization Process and Stability of Octadentate Eu(III) 1,2-HOPO Complexes

Anthony D'Aléo, Evan G. Moore, Jide Xu, Lena J. Daumann, and Kenneth N. Raymond*

Department of Chemistry, University of California, Berkeley, California 94720-1460, United States

Chemical Sciences Division, Lawrence Berkeley National Laboratory, Berkeley, California 94720, United States

Supporting Information

**ABSTRACT:** The synthesis of a series of octadentate ligands containing the 1-hydroxypyridin-2-one (1,2-HOPO) group in complex with europium(III) is reported. Within this series, the central bridge connecting two diethylenetriamine units linked to two 1,2-HOPO chromophores at the extremities (5-LIN-1,2-HOPO) is varied from a short ethylene chain (H(2,2)-1,2-HOPO) to a long pentaethylene oxide chain (H(17O5,2)-1,2-HOPO). The thermodynamic stability of the europium complexes has been studied and reveals these complexes may be effective for biological measurements. Extension of the central bridge results in exclusion of the inner-sphere water molecule observed for $[Eu(H(2,2)\text{-}1,2\text{-}HOPO)]^-$ going from a nonacoordinated to an octacoordinated Eu(III) ion. With the longer chain length ligands, the complexes display increased luminescence properties in aqueous medium with an optimum of 20% luminescence quantum yield for the $[Eu(H(17O5,2)\text{-}1,2\text{-}HOPO)]^-$ complex. The luminescence properties for $[Eu(H(14O4,2)\text{-}1,2\text{-}HOPO)]^-$ and $[Eu(H(17O5,2)\text{-}1,2\text{-}HOPO)]^-$ are better than that of the model bis-tetradentate $[Eu(5LIN^{Me}\text{-}1,2\text{-}HOPO)_2]^-$ complex, suggesting a different geometry around the metal center despite the geometric freedom allowed by the longer central chain in the H(*m*O*n*,2) scaffold. These differences are also evidenced by examining the luminescence spectra at room temperature and at 77 K and by calculating the luminescence kinetic parameters of the europium complexes.

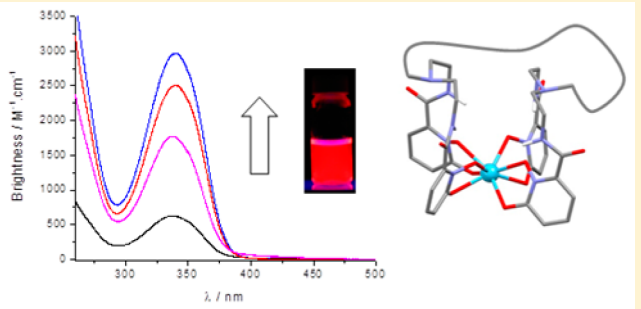


## INTRODUCTION

The dangers and drawbacks inherent with radioactivity-based biological assay methods together with the low sensitivity of MRI agents have yielded a major shift toward luminescence measurements and visualization techniques due to their demonstrated and dramatically increased sensitivity.[1−3] In such techniques, the low background signal and the wide variety of detection wavelengths make these measurements highly appealing.[3] For coordination compounds to be utilized for biological luminescence purposes, several parameters have to be optimized.[4−7] First, the observed emission should display insensitivity toward the environment. This is especially important for labeling applications with biomolecules. Furthermore, in addition to high thermodynamic and kinetic stability, to prevent unwanted release of metal, the complex should have high overall luminescence quantum yield and brightness. The latter parameter can be determined from the product of the luminescence quantum yield and the molar absorption coefficient. In this respect, lanthanide ions are appealing since they possess intrinsic long-lived excited state lifetimes and can be tuned to have high luminescence quantum yields.[8−10] For these reasons, their use has now spread to traditional clinical environments,[11] and applications have grown from their more traditional use as chemical shift reagents[12−14] toward clinical assays for DNA sequencing,[10] for antioxidant detection,[15,16] and for use in high-throughput screening.[17,18] For instance, several Ln(III) chelates (with Ln = Tb or Eu) are commercially available (e.g., Lance, PerkinElmer; LanthaScreen, Invitrogen, CisBio), and fluorescent assay platforms such as Dissociation-Enhanced Lanthanide Fluorescent Immuno-Assay (DELFIA)[19] are well developed, offering increased sensitivity compared to colorimetric assay formats such as the Enzyme-Linked Immuno-Sorbent Assay (ELISA).[20] Since these complexes are also expected to be useful in FRET-type experiments,[21] high brightness together with good aqueous solubility and stability are an added requirement.[10,22,23]

It has been shown that octadentate 1-hydroxypyridin-2-one (1,2-HOPO) ligands hold high promise for biological applications and in radionuclide decorporation.[24−28] Here, we report on the synthesis, thermodynamic stability, and photophysical properties of several octadentate 1,2-HOPO derivatives with the aim of increasing the luminescent properties of the respective Eu(III) complexes in aqueous solution. The ligands are composed of two diethylamine units which bridge two 1,2-HOPO moieties connected by a tertiary nitrogen atom (e.g., $5LIN^{Me}$-1,2-HOPO). For the octadentate ligands, two of such units are connected by either aliphatic or oligo-ethylene

**Received:** April 2, 2015
**Published:** July 7, 2015

  

DOI: 10.1021/acs.inorgchem.5b00748
*Inorg. Chem.* 2015, 54, 6807−6820

**Scheme 1. Synthesis of H(*m*,2)-1,2-HOPO[a]**

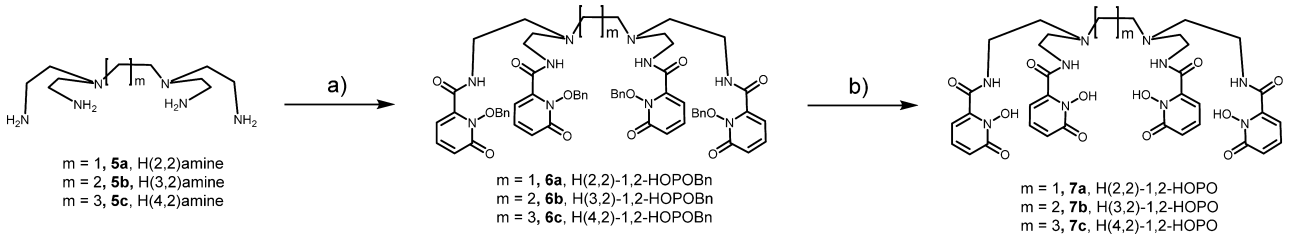


[a]Reagents and conditions: (a) 1,2-HOPOBn-thiaz, $Et_3N$, DCM, RT, 16 h; (b) conc HCl/glacial HOAc (1:1), 3 days, RT.

**Scheme 2. Synthesis of H(*m*O*n*,2)-1,2-HOPO[a]**

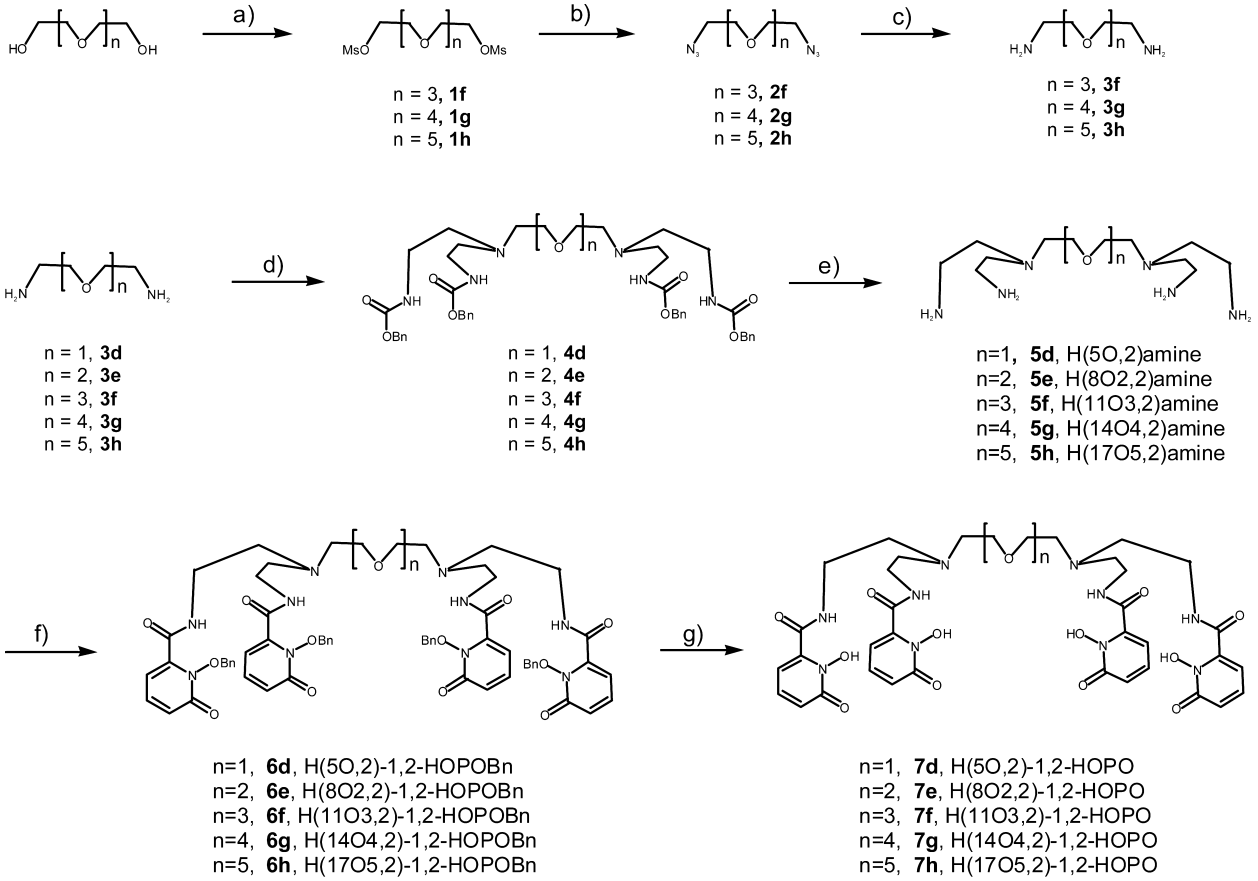


[a]Reagents and conditions: (a) MsCl, $Et_3N$, DCM, 0 °C to RT, 4 h; (b) $NaN_3$, EtOH, 80 °C, 16 h; (c) $H_2$ (500 psi), 5−10% Pd/C, 8 h; (d) *Z*-aziridine, *tert*-butyl alcohol, 80 °C, 16 h; (e) $H_2$ (500 psi), 5−10% Pd/C, 8 h; (f) 1,2-HOPOBn acid chloride, $K_2CO_3$, $H_2O$/DCM biphasic, 8 h; (g) conc HCl/glacial HOAc (1:1), 3 days, RT.

glycol chains (resulting in four 1,2-HOPO units which compose the octadentate ligand topology). The stability of such complexes has been determined and shows that these complexes are stable in aqueous medium, allowing measurements at submicromolar concentration. The luminescence properties in terms of their molar absorption coefficients, luminescence quantum yields, luminescence lifetimes, and brightness are investigated, together with the pattern of the Eu(III) emission spectra both at room temperature and at 77 K.

## EXPERIMENTAL SECTION

**General.** All of the reagents and solvents used were of analytical grade and purchased commercially; H(2,2)-1,2-HOPO and 5LIN$^{Me}$-1,2-HOPO were prepared as reported elsewhere.[29] Thin-layer chromatography (TLC) was performed using precoated Kieselgel 60 F254 plates. Flash chromatography was performed using EM Science Silica Gel 60 (230−400 mesh). NMR spectra were obtained using either a Bruker AM-300 or a DRX-500 spectrometer operating at 300 (75) and 500 (125) MHz for $^1H$ (or $^{13}C$), respectively. $^1H$ (or $^{13}C$) chemical shifts are reported in ppm relative to the solvent resonances, taken as $\delta$ 7.26 ($\delta$ 77.0), $\delta$ 2.49 ($\delta$ 39.5), and $\delta$ 3.31 $\delta$ (49.0), respectively, for $CDCl_3$, $(CD_3)_2SO$, and $CD_3OD$, while coupling constants ($J$) are reported in Hertz. The following standard abbreviations are used for characterization of $^1H$ NMR signals: s = singlet, d = doublet, t = triplet, q = quartet, quin = quintet, m = multiplet, dd = doublet of doublets. Both low-resolution mass (FAB) and high-resolution mass (HRESI) spectra were obtained from the Micromass/Analytical Facility operated by the College of Chemistry, University of California, Berkeley, CA. Elemental analyses were performed by the Microanalytical Laboratory, University of California, Berkeley, CA.



DOI: 10.1021/acs.inorgchem.5b00748
*Inorg. Chem.* 2015, 54, 6807−6820

*CAUTION! Some of the syntheses reported herein involve the use of organic azides. These are potentially explosive, and appropriate care should be taken when handling the respective compounds.*

**Synthesis.** The syntheses of H(*m*,2)-1,2-HOPO and H(*m*On,2)-1,2-HOPO ligands are shown in Schemes 1 and 2, respectively.

*H(3,2)-1,2-HOPOBn (**6b**).* To a solution of 1,2-HOPOBn-thiazolide[26] (1.38 g, 4 mmol) and $Et_3N$ (0.4 g, 4 mmol) in dry dichloromethane (30 mL) was added neat H(3,2)-amine (**5b**) (220 mg, 0.9 mmol). The mixture was stirred overnight, the solvent was then removed, and the residue was loaded onto a flash silica column. Elution with 2−6% methanol in dichloromethane allows the separation of the benzyl-protected precursor as pale yellow oil (0.73 g, 71% based on amine). $^1$H NMR (500 MHz, $CDCl_3$): $\delta$ 1.03 (s, 2H), 1.87 (s, 4H), 2.13 (s, 8H), 3.08 (s, br, 8H), 5.22 (s, 8H), 6.15 (d, $J$ = 6 Hz, 4H), 6.52 (d, $J$ = 9 Hz, 4H), 7.15 (t, $J$ = 9 Hz, 4H), 7.30−7.34 (m, 12H), 7.44 (m, 8H), 7.49 (s, 4H). $^{13}$C NMR (125 MHz, $CDCl_3$): $\delta$ 25.3, 37.6, 51.2, 52.8, 79.4, 105.2, 123.5, 128.5, 129.4, 133.2, 138.1, 142.9, 158.4, 160.7, 162.2. MS (FAB+) ($m/z$): calcd for $[C_{63}H_{67}N_{10}O_{12}]^+$ 1155.6, found 1155.6.

*H(3,2)-1,2-HOPO (**7b**).* Compound **6b** (0.87 g, 0.75 mmol) was dissolved in concentrated HCl (12 M)/glacial acetic acid (1:1, 20 mL) and stirred at room temperature for 3 days. Filtration followed by removal of the solvent gives a beige residue, which was washed with ether to give the product (0.52 g, 87%) as a beige solid. $^1$H NMR (500 MHz, DMSO-$d_6$): $\delta$ 1.67 (s, br, 2H), 2.70−2.85 (m, 12H), 3.07 (s, br, 4H), 5.97 (dd, $J$ = 6 Hz, 4H), 6.02 (dd, $J$ = 9 Hz, 4H), 6.67 (dd, $J$ = 9 Hz, 4H). $^{13}$C NMR (500 MHz, $CD_3OD$): $\delta$ 20.5, 36.3, 51.7, 54.7, 109.9, 121.5, 138.8, 140.7, 160.3, 163.8. Anal. Calcd for $C_{35}H_{42}N_{10}O_{12}\cdot 2HCl\cdot 1.5H_2O$: C, 46.98; H, 5.29; N, 15.66. Found: C, 47.19; H, 5.22; N, 15.55. MS (ESI$^-$) ($m/z$): calcd for $[C_{35}H_{41}N_{10}O_{12}]^-$ 793.3, found 793.1.

*H(4,2)-1,2-HOPOBn (**6c**).* This compound was prepared by the similar procedure as compound **6b**, except H(4,2) amine (**5c** 234 mg, 0.9 mmol) was used instead of H(3,2) amine (**5b**). Separation and purification were performed as described above. The benzyl-protected precursor was obtained as a pale yellow oil (0.72 g, 68% based on amine). $^1$H NMR (500 MHz, $CDCl_3$): $\delta$ 0.85 (s, 4H), 1.95 (s, 4H), 2.29 (s, 8H), 3.15 (s, br, 8H), 5.24 (s, 8H), 6.18 (s, 4H), 6.50 (d, $J$ = 9 Hz, 4H), 7.14 (m,4H), 7.30−7.34 (m, 12H), 7.43−7.50 (m, 12H). $^{13}$C NMR (125 MHz, $CDCl_3$): $\delta$ 23.9, 37.4, 52.1, 53.0, 78.8, 105.0, 122.9, 128.1, 128.9, 129.7, 133.1, 137.8, 142.9, 158.1, 160.3. MS (FAB+) ($m/z$): calcd for $[C_{64}H_{69}N_{10}O_{12}]^+$ 1169.5, found 1169.5.

*H(4,2)-1,2-HOPO (**7c**).* Compound **6c** (0.49 g, 0.42 mmol) was deprotected with concentrated HCl (12 M)/glacial acetic acid (1:1) as described for deprotection of **6b**. Compound **7c** was obtained as a beige solid (0.36 g, 90%). $^1$H NMR (500 MHz, DMSO-$d_6$): $\delta$ 1.81 (s, br, 4H), 3.15 (s, 4H), 3.25 (s, 8H), 3.55 (s, 8H), 6.43 (d, $J$ = 6 Hz, 4H), 6.59 (d, $J$ = 9 Hz, 4H), 7.40 (d, $J$ = 9 Hz, 4H), 9.13 (t, $J$ = 5.6 Hz, 4H), 10.96 (s, br, 4H). $^{13}$C NMR (100 MHz, $CD_3OD$): $\delta$ 22.1, 36.3, 49.8, 54.3, 109.7, 121.7, 139.1, 140.9, 160.3, 163.7. Anal. Calcd for $C_{36}H_{44}N_{10}O_{12}\cdot 2HCl\cdot 2.5H_2O$: C, 46.78; H, 5.56; N, 15.15. Found: C, 46.82; H, 5.23; N, 14.89. MS (ESI$^-$) ($m/z$): calcd for $[C_{36}H_{43}N_{10}O_{12}]^-$ 807.3, found 807.3.

*H(5O,2)-CBZ (**4d**).* 2,2′-Oxybis(ethan-1-amine) (5LIO-amine) (0.21 g, 2 mmol) and benzyl aziridine-1-carboxylate (1.77 g, 10 mmol) were mixed in *tert*-butanol (30 mL) at room temperature under $N_2$. The mixture was stirred under an $N_2$ atmosphere at 80 °C for 16 h, when TLC showed the completeness of the reaction. The volatiles were removed under vacuum, and the residue was dissolved in dichloromethane. The appropriate fractions of a gradient flash silica gel column (1−7% methanol in dichloromethane) were collected and evaporated to dryness to give a pale beige thick oil. Yield: 1.28 g, 79%. $^1$H NMR (300 MHz, $CDCl_3$): $\delta$ 2.53 (s, br, 12H), 3.17 (s, br, 4H), 3.83 (s, br, 8H), 5.04 (s, br, 8H), 7.29 (s, br, 20H). $^{13}$C NMR (75 MHz, $CDCl_3$): $\delta$ 38.8, 53.0, 53.6, 69.3, 128.0, 128.1, 128.4, 136.6, 156.4. MS (FAB+) ($m/z$): calcd for $[C_{44}H_{57}N_6O_9]^+$ 813.4, found 813.5.

*H(5O,2)-Amine (**5d**).* H(5O,2)CBZ (**4d** 0.83 g, 1 mmol) and 0.1 g of 5% Pd/C catalyst were combined in methanol (25 mL). The mixture was hydrogenated (500 psi pressure, room temperature) overnight in a Parr bomb. After removing the catalyst by filtration, the filtrate was evaporated to dryness to leave a pale yellow oil as product. Yield: 0.23 g (84%). $^1$H NMR (500 MHz, $CDCl_3$): $\delta$ 0.84 (t, $J$ = 5 Hz, 4H), 0.90 (t, $J$ = 5 Hz, 8H), 1.10 (t, $J$ = 5 Hz, 8H), 1.66 (t, $J$ = 5 Hz, 4H). $^{13}$C NMR (125 MHz, $CDCl_3$): $\delta$ 38.6, 53.4, 53.9, 70.1. MS (FAB +) ($m/z$): calcd for $[C_{12}H_{33}N_6O]^+$ 277.3, found 277.3.

*H(5O,2)-1,2-HOPOBn (**6d**).* To a mixture of compound **5d** (0.14 g, 0.5 mmol) and 30% potassium carbonate solution (5 mL) in dichloromethane (20 mL) with cooling by an ice bath, a solution of 1,2-HOPOBn acid chloride from 0.75 g (3 mmol) of 1,2-HOPOBn acid in dry dichloromethane (35 mL) was added dropwise in 2 h with vigorous stirring. The mixture was warmed to room temperature with stirring, until TLC indicated the reaction was complete. The organic phase was separated and loaded on a flash silica column. Elution with 2−7% methanol in dichloromethane allows the separation of the benzyl-protected precursor H(5O,2)-1,2-HOPOBn (0.42g, 71% based on the free amine) as a thick pale yellow oil. $^1$H NMR (300 MHz, $CDCl_3$): $\delta$ 2.14 (s, 4H), 2.32 (s, 8H), 2.83 (s, 4H), 3.06 (s, 8H), 5.15 (s, 8H), 6.05 (s, 4H), 6.34 (s, 4H), 7.04 (s, 4H), 7.20 (s, 12H), 7.32 (s, 8H). 7.63 (s, 4H). $^{13}$C NMR (75 MHz, $CDCl_3$): $\delta$ 37.3, 52.0, 52.7, 78.8, 104.8, 122.9, 128.1, 128.9, 129.7, 133.1, 138.0, 143.0, 158.1, 160.3. MS (FAB+) ($m/z$): calcd for $[C_{64}H_{69}N_{10}O_{13}]^+$ 1185.5, found 1185.6.

*H(5O,2)-1,2-HOPO (**7d**).* H(5O,2)-1,2-HOPOBn was deprotected with concentrated HCl (12 M)/glacial acetic acid (1:1) as mentioned above for deprotecting **6b**. The ligand was obtained as a beige solid. Yield: 81%. $^1$H NMR (500 MHz, DMSO-$d_6$): $\delta$ 3.40 (s, 8H), 3.52 (s, 4H), 3.70 (s, 8H), 3.86 (s, 4H), 6.41 (d, $J$ = 6 Hz, 4H), 6.60 (d, $J$ = 9 Hz, 4H), 7.40 (d, $J$ = 9 Hz, 4H), 9.11 (t, 2H, $J$ = 6 Hz), 10.48 (s, 4H). $^{13}$C NMR (75 MHz, $CD_3OD$): $\delta$ 36.7, 55.0, 55.4, 66.3, 110.1, 121.6, 138.9, 141.4, 160.6, 163.9. Anal. Calcd for $C_{36}H_{44}N_{10}O_{13}\cdot 2HCl\cdot H_2O$: C, 47.22; H, 5.28; N, 15.30. Found: C, 47.54; H, 5.35; N, 14.95. MS (FAB+) ($m/z$): calcd for $[C_{36}H_{45}N_{10}O_{13}]^+$ 825.3, found 825.3.

*H(8O2,2)-CBZ (**4e**).* This compound was prepared by the similar procedure as described for compound **4d** except 2-[2-(2-amino-ethoxy)-ethoxy]-ethylamine (0.15 g, 1 mmol) was used instead of 5LIO-amine. Separation and purification were performed as described above. H(8O2,2)-CBZ was obtained as a pale beige thick oil. Yield: 0.64 g, 74%. $^1$H NMR (300 MHz, $CDCl_3$): $\delta$ 2.53 (s, 12H), 3.16 (s, 8H), 3.23 (s, 4H), 3.35 (s, 4H), 5.03 (s, 8H), 7.28 (s, 20H). $^{13}$C NMR (75 MHz, $CDCl_3$): $\delta$ 38.8, 52.6, 53.6, 66.3, 69.2, 69.9, 127.8, 128.0, 128.3, 136.6, 156.5. MS (FAB+) ($m/z$): calcd for $[C_{46}H_{61}N_6O_{10}]^+$ 857.4, found 857.5.

*H(8O2,2)-Amine (**5e**).* This compound was prepared by the similar procedure for preparing compound **5d** except compound **4e** (0.86 g, 1 mmol) was used instead of compound **4d**. A pale yellow oil was obtained as the product, yield 0.27 g (85%). $^1$H NMR (300 MHz, $D_2O$): $\delta$ 2.49 (t, $J$ = 5 Hz, 4H), 2.54 (t, $J$ = 5 Hz, 8H), 2.78 (t, $J$ = 5 Hz, 8H), 3.34 (t, $J$ = 5 Hz, 4H), 3.40 (t, $J$ = 5 Hz, 4H); $^{13}$C NMR (125 MHz, $D_2O$): $\delta$ 36.9, 51.3, 51.7, 68.1, 69.3; MS (FAB+) ($m/z$): Calcd for $[C_{14}H_{37}N_6O_2]^+$ 321.3, Found: 321.3

*H(8O2,2)-1,2-HOPOBn (**6e**).* This compound was prepared by a similar procedure for preparing compound **6d**, except compound **5e** (0.5 mmol) was used instead of compound **5d**. Separation and purification were performed as described above. The benzyl-protected precursor **6e** (0.41g, 68% based on the free amine) was obtained as a thick pale yellow oil. $^1$H NMR (300 MHz, $CDCl_3$): $\delta$ 2.31 (s, 4H), 2.42 (s, 8H), 2.63 (s, 4H), 2.85 (s, 4H), 3.14 (s, 8H), 5.32 (s, 8H), 6.20 (d, $J$ = 6 Hz, 4H), 6.48 (d, $J$ = 9 Hz, 4H), 7.08 (s, 4H), 7.34 (s, 16H), 7.50 (s, 8H). $^{13}$C NMR (75 MHz, $CDCl_3$): $\delta$ 37.4, 52.2, 53.0, 68.8, 69.0, 79.0, 104.9, 123.0, 129.1, 130.1, 133.3, 138.2, 143.2, 158.2, 160.4. MS (FAB+) ($m/z$): calcd for $[C_{66}H_{73}N_{10}O_{14}]^+$ 1229.5, found 1229.7.

*H(8O2,2)-1,2-HOPO (**7e**).* Compound **6e** was deprotected with concentrated HCl (12 M)/glacial acetic acid (1:1) as mentioned above for preparing compound **7b**. An off-white solid was obtained as product. Yield: 80%. $^1$H NMR (500 MHz, DMSO-$d_6$): $\delta$ 3.36 (s, 8H), 3.47 (s, 4H), 3.62 (s, 4H), 3.67 (q, $J$ = 5 Hz, 8H), 3.85 (s, 4H), 6.43 (dd, $J$ = 6 Hz, 4H), 6.60 (d, $J$ = 9 Hz, 4H), 7.41 (d, $J$ = 9 Hz, 4H), 9.11 (t, $J$ = 5.6 Hz, 2H), 10.56 (s, 4H). $^{13}$C NMR (125 MHz, $CD_3OD$): $\delta$ 36.4, 49.3, 55.0, 66.0, 71.5, 110.2, 121.0, 139.0, 141.1, 159.9, 163.2.



DOI: 10.1021/acs.inorgchem.5b00748
*Inorg. Chem.* 2015, 54, 6807−6820

Anal. Calcd for $C_{38}H_{48}N_{10}O_{14}\cdot 2HCl\cdot 2H_2O$: C, 46.68; H, 5.57; N, 14.32. Found: C, 46.69; H, 5.71; N, 13.98. MS (FAB+) ($m/z$): calcd for $[C_{38}H_{49}N_{10}O_{14}]^+$ 869.3, found 869.3.

*Tetraethylene Glycol Dimesylate (**1f**).* To a solution of 3.9 g (20 mmol) of tetraethylene glycol and 4 g of $Et_3N$ (2.0 equiv) in dry dichloromethane (30 mL) at 0 °C under $N_2$ atmosphere was added 3 mL of methanesulfonyl chloride in dry dichloromethane (10 mL) via a Teflon cannula with a glass capillary tip over 30 min. The reaction mixture was stirred at this temperature for 4 h and then treated with 30 mL of a cold saturated aqueous $NaHCO_3$ solution. The mixture was extracted with 3 × 30 mL of dichloromethane. The combined organic layers were dried ($MgSO_4$) and evaporated to give a crude product that was purified by column chromatography (2−7% methanol/dichloromethane). Yield: 6.3 g (90%) colorless thick oil. $^1$H NMR (300 MHz, $CDCl_3$): $\delta$ 3.06 (s, 6H), 3.63 (m, 8H), 4.18 (m, 4H). $^{13}$C NMR (75 MHz, $CDCl_3$): $\delta$ 36.8, 68.2, 69.1, 69.7, 69.8. MS (FAB+) ($m/z$): calcd for $[C_{10}H_{23}O_9S_2]^+$ 351.1, found 351.1.

*Tetraethylene Glycol Diazide (**2f**).* A solution of **1f** (3.5 g, 10 mmol) and sodium azide (2.2 equiv) in 50 mL of ethanol was heated at reflux for 8 h. After cooling to room temperature, the ethanol was removed in vacuo, and the remaining mixture was diluted with 100 mL of dichloromethane. The solution was washed twice with water (50 mL), dried over anhydrous sulfate, and concentrated in vacuo to give the crude product, which was purified by silica gel chromatography eluting with a gradient of 2−5% methanol in dichloromethane to afford the product as colorless oil (1.9 g). Yield: 77% based on dimesylate. $^1$H NMR (300 MHz, $CDCl_3$): $\delta$ 3.39 (t, $J$ = 4.8 Hz, 4H), 3.65 (m, 12H). $^{13}$C NMR (75 MHz, $CDCl_3$): $\delta$ 50.2, 69.6, 70.2. MS (FAB+) ($m/z$): calcd for $[C_8H_{16}N_6O_3]^+$ 245.1, found 245.1.

*Tetraethylene Glycol Diamine (**3f**).* The tetraethylene glycol diazide (1.9 g) was dissolved in 40 mL of ethanol and hydrogenated at 0−5 °C (cooling with a water bath) and 500 psi in the presence of 10% Pd/C (0.3 g). Filtration of the catalyst and evaporation of the solvent gave 1.3 g (90%) of compound **3f**. $^1$H NMR (300 MHz, $CDCl_3$): $\delta$ 1.60 (s, 4H), 2.81 (m, 4H), 3.45 (m, 12H), 3.57 (m, 12H). $^{13}$C NMR (75 MHz, $CDCl_3$): $\delta$ 41.3, 69.1, 69.8, 72.9. MS (FAB+) ($m/z$): calcd for $[C_8H_{21}N_2O_3]^+$ 193.2, found 193.1.

*H(11O3,2)-Cbz (**4f**).* This compound was prepared by the similar procedure as described for compound **4d**, except tetraethylene glycol diamine (0.39 g, 2 mmol) was used instead of 5LIO-amine. Separation and purification were performed as described above. H(11O3,2)-Cbz was obtained as a beige thick oil. Yield: 1.4 g, 79%. $^1$H NMR (300 MHz, $CDCl_3$): $\delta$ 2.53 (s, 12H), 3.17 (s, 4H), 3.83 (s, 8H), 5.04 (s, 8H), 7.29 (s, 20H). $^{13}$C NMR (75 MHz, $CDCl_3$): $\delta$ 38.8, 50.0, 53.8, 66.0, 69.3, 69.9, 127.6, 127.7, 128.1, 136.5, 156.5. MS (FAB+) ($m/z$): calcd for $[C_{48}H_{65}N_6O_{11}]^+$ 901.5, found 901.6.

*H(11O3,2)-Tetraamine (**5f**).* H(11O3,2)-Cbz (0.9 g, 1 mmol) was dissolved in 30 mL of methanol and hydrogenated at 25 °C and 500 psi in the presence of 10% Pd/C (0.2 g). Filtration of the catalyst and evaporation of the solvent gave 0.30 g (90%) of H(11O3,2)-tetraamine. $^1$H NMR (400 MHz, $D_2O$): $\delta$ 2.68 (s, 4H), 2.80 (t, $J$ = 5 Hz, 8H), 3.09 (t, $J$ = 5 Hz, 8H), 3.50 (s, 4H), 3.65 (s, 8H). $^{13}$C NMR (100 MHz, $D_2O$): $\delta$ 39.7, 54.1, 54.5, 71.0, 72.0. MS (FAB+) ($m/z$): calcd for $[C_{16}H_{41}N_6O_3]^+$ 365.3, found 365.3.

*H(11O3,2)-1,2-HOPOBn (**6f**).* This compound was prepared by the similar procedure as described for compound **6d**, except compound **5f** (0.5 mmol) was used instead of compound **5d**. Separation and purification were performed as described above. Compound **6f** was obtained as a thick pale yellow oil. Yield: 0.48 g, 75% based on the free amine. $^1$H NMR (500 MHz, $CDCl_3$): $\delta$ 2.32 (s, 4H), 2.46 (m, 8H), 3.00 (m, 8H), 3.03 (s, 4H), 3.06 (s, 4H), 3.18 (m, 8H), 5.30 (s, 8H), 6.15 (d, $J$ = 7 Hz, 4H), 6.52 (d, $J$ = 9 Hz, 4H), 7.17 (d, $J$ = 9.0 Hz, 4H), 7.32 (m, 12H), 7.49 (m, 8H). $^{13}$C NMR (125 MHz, $CDCl_3$): $\delta$ 37.4, 52.3, 53.1, 53.3, 69.1, 69.3, 69.6, 78.8, 104.6, 122.9, 128.1, 128.9, 129.6, 137.9, 143.1, 158.1, 160.5. MS (FAB+) ($m/z$): calcd for $[C_{69}H_{77}N_{10}O_{15}]^+$ 1273.6, found 1273.2.

*H(11O3,2)-1,2-HOPO (**7f**).* Compound **6f** was deprotected with concentrated HCl (12 M)/glacial acetic acid (1:1) as mentioned above for compound **7b**. An off-white solid was obtained as product. Yield: 85%. $^1$H NMR (300 MHz, DMSO-$d_6$): $\delta$ 3.38 (s, 8H), 3.45 (s, 4H), 3.56 (s, 8H), 3.65 (s, 8H), 3.82 (s, 4H), 6.41 (d, $J$ = 7.0 Hz, 4H), 6.61 (d, $J$ = 9.0 Hz, 4H), 7.41 (d, $J$ = 8.0 Hz, 4H), 9.09 (s, 4H). $^{13}$C NMR (75 MHz, $CD_3OD$): $\delta$ 36.5, 54.9, 66.1, 71.3, 71.5, 111.7, 120.7, 140.4, 141.8, 160.0, 162.9. Anal. Calcd for $C_{40}H_{52}N_{10}O_{15}\cdot 2HCl\cdot 5H_2O$: C, 44.65; H, 5.99; N, 13.02. Found: C, 44.63; H, 5.98; N, 12.74. MS (FAB+) ($m/z$): calcd for $[C_{40}H_{53}N_{10}O_{15}]^+$ 913.4, found 913.3.

*Pentaethylene Glycol Dimesylate (**1g**).* This compound was prepared by the similar procedure as described for compound **1f**, except pentaethylene glycol (0.5 mmol) was used instead of tetraethylene glycol. Separation and purification were performed as described above. A pale yellow thick oil was obtained as product. Yield: 90%. $^1$H NMR (300 MHz, $CDCl_3$): $\delta$ $\delta$ 3.09 (s, 6H), 3.64 (m, 12H), 3.77 (m, 4H), 4.38 (m, 4H). $^{13}$C NMR (75 MHz, $CDCl_3$): $\delta$ 37.4, 67.8, 69.0, 69.8, 69.9. MS (FAB+) ($m/z$): calcd for $[C_{12}H_{27}O_{10}S_2]^+$ 395.1, found 395.1.

*Pentaethylene Glycol Diazide (**2g**).* This compound was prepared by the similar procedure as described for compound **2f**, except pentaethylene glycol dimesylate was used instead of tetraethylene glycol dimesylate. Separation and purification were performed as described above. Colorless thick oil was obtained as product. Yield: 77% based dimesylate. $^1$H NMR (300 MHz, $CDCl_3$): $\delta$ 3.34 (t, $J$ = 5 Hz, 4H), 3.62 (m, 16H). $^{13}$C NMR (75 MHz, $CDCl_3$): $\delta$ 50.5, 69.9, 70.5. MS (FAB+) ($m/z$): calcd for $[C_{10}H_{21}N_6O_4]^+$ 289.2, found 289.2.

*Pentaethylene Glycol Diamine (**3g**).* Compound **3g** was prepared by catalytical hydrogenation as described for compound **5f**, except compound **2g** was used instead of **2f**. Yield: 80%. $^1$H NMR (300 MHz, $CDCl_3$): $\delta$ 1.11 (s, 4H), 2.52 (t, $J$ = 5 Hz, 4H), 3.17 (t, $J$ = 5 Hz, 4H), 3.33 (m, 12H). $^{13}$C NMR (75 MHz, $CDCl_3$): $\delta$ 41.3, 69.1, 69.8, 72.9. MS (FAB+) ($m/z$): Calcd for $[C_{10}H_{25}N_2O_4]^+$ 237.2, Found: 237.2.

*H(14O4,2)-Cbz (**4g**).* This compound was prepared by the similar procedure as described for preparing compound **4d**, except pentaethylene glycol diamine (0.47 g, 2 mmol) was used instead of 5LIO-amine. Separation and purification were performed as described abve. Compound **4g** was obtained as a beige thick oil. Yield: 1.5 g (79% based on diamine). $^1$H NMR (300 MHz, $CDCl_3$): $\delta$ 2.60 (t, $J$ = 5 Hz, 12H), 3.18 (t, $J$ = 5 Hz, 8H), 3.40 (m, 6H), 3.44 (s, 8H), 5.04 (s, 8H), 5.80 (s, 4H), 7.27 (s, 20H). $^{13}$C NMR (300 MHz, $CDCl_3$): $\delta$ 38.9, 52.8, 53.3, 66.0, 66.2, 69.9, 70.1, 70.2, 127.7, 127.9, 128.2, 136.6, 156.6. MS (FAB+) ($m/z$): calcd for $[C_{50}H_{69}N_6O_{12}]^+$ 945.5, found 945.5.

*H(14O4,2)-Amine (**5g**).* H(14O4,2)CBZ (0.95 g, 1 mmol) was deprotected by catalytic hydrogenation as described for preparing compound **5e**. A 0.37 g (90%) amount of H(14O4,2)-amine was obtained as a colorless thick oil. $^1$H NMR (400 MHz, $D_2O$): $\delta$ 2.70 (s, 4H), 2.82 (t, $J$ = 5 Hz, 8H), 3.12 (t, $J$ = 5 Hz, 8H), 3.56 (s, 4H), 3.70 (s, 8H). $^{13}$C NMR (100 MHz, $D_2O$): $\delta$ 39.2, 55.1, 58.5, 69.0, 71.0, 72.0. MS (FAB+) ($m/z$): calcd for $[C_{18}H_{45}N_6O_4]^+$ 409.4, found 409.3.

*H(14O4,2)-1,2-HOPOBn (**6g**).* This compound was prepared by the similar procedure as described for preparing compound **6d**, except compound **5g** (0.21 g, 0.5 mmol) was used instead of compound **5d**. Separation and purification were performed as described above. Compound **6g** was obtained as a pale yellow thick oil. Yield: 0.49 g (75% based on the free amine). $^1$H NMR (500 MHz, $CDCl_3$): $\delta$ 2.21 (s, 4H), 2.48 (s, 8H), 3.11 (m, 12H), 3.19 (s, 12H), 5.28 (s, 8H), 6.16 (d, $J$ = 7 Hz, 4H), 6.54 (d, $J$ = 9 Hz, 4H), 7.17 (dd, $J$ = 9 Hz, 4H), 7.32 (m, 12H), 7.49 (m, 12H). $^{13}$C NMR (100 MHz, $CDCl_3$): $\delta$ 37.6, 52.1, 53.1, 53.3, 69.2, 69.7, 77.2, 78.8, 104.6, 122.9, 128.1, 128.8, 129.8, 133.3, 137.9, 143.1, 158.1, 160.5. MS (FAB+) ($m/z$): calcd for $[C_{70}H_{81}N_{10}O_{16}]^+$ 1317.6, found 1317.4.

*H(14O4,2)-1,2-HOPO (**7g**).* H(14O4,2)-1,2-HOPOBn was deprotected with concentrated HCl (12 M)/glacial acetic acid (1:1) as mentioned above for compound **7b**. An off-white foam was obtained as product. Yield: 90%. $^1$H NMR (300 MHz, $CD_3OD$): $\delta$ 3.26 (s, 4H), 3.28 (s, 4H), 3.56 (s, 8H), 3.38 (m, 16H), 3.66 (s, 8H), 3.72 (s, 4H), 6.57 (d, $J$ = 8 Hz, 8H), 7.28 (d, $J$ = 8 Hz, 4H). $^{13}$C NMR (75 MHz, $CD_3OD$): $\delta$ 36.5, 54.9, 55.1, 66.0, 67.0, 71.3, 71.4, 109.8, 121.4, 138.9, 141.2, 160.1, 163.4. Anal. Calcd for $C_{42}H_{56}N_{10}O_{16}\cdot 2HCl\cdot 4H_2O$: C, 45.78; H, 6.04; N, 12.71. Found: C, 45.52; H, 5.95; N, 12.47. MS (FAB+) ($m/z$): calcd for $[C_{42}H_{57}N_{10}O_{16}]^+$ 956.4, found 956.3.

*Hexaethylene Glycol Dimesylate (**1h**).* This compound was prepared by the similar procedure as described for compound **1f**,



DOI: 10.1021/acs.inorgchem.5b00748
*Inorg. Chem.* 2015, 54, 6807−6820

except hexaaethylene glycol (0.5 mmol) was used instead of tetraethylene glycol. Separation and purification were performed as described above. A pale yellow thick oil was obtained as product. Yield: 90%. $^1$H NMR (300 MHz, $CDCl_3$): $\delta$ 3.03 (s, 6H), 3.56 (s, 8H), 3.60 (m, 6H), 3.70 (m, 4H), 4.32 (m, 4H). $^{13}$C NMR (75 MHz, $CDCl_3$): $\delta$ 37.4, 67.8, 69.0, 69.8, 69.9. MS (FAB+) ($m/z$): calcd for $[C_{14}H_{31}O_{11}S_2]^+$ 439.1, found 439.1.

*Hexaethylene Glycol Diazide (**2h**).* This compound was prepared by the similar procedure as described for compound **2f**, except hexaethylene glycol dimesylate was used instead of tetraethylene glycol dimesylate. Separation and purification were performed as described above. A colorless thick oil was obtained as product (yield 75% based on dimesylate). $^1$H NMR (300 MHz, $CDCl_3$): $\delta$ 3.36 (m, 4H), 3.65 (m, 20H). $^{13}$C NMR (75 MHz, $CDCl_3$): $\delta$ 50.0, 69.4, 69.9, 70.0. MS (FAB+) ($m/z$): calcd for $[C_{12}H_{25}N_6O_5]^+$ 333.2, found: 333.2.

*Hexaethylene Glycol Diamine (**3h**).* Compound **3h** was prepared by catalytic hydrogenation as for preparing compound **5f**, except compound **2h** was used instead of **2f**. Yield: 82% $^1$H NMR (300 MHz, $CDCl_3$): $\delta$ 1.11 (s, 4H), 2.80 (t, $J$ = 5 Hz, 4H), 3.45 (t, $J$ = 5 Hz, 4H), 3.58 (m, 16H). $^{13}$C NMR (75 MHz, $CDCl_3$): $\delta$ 40.8, 69.2, 69.5, 69.6, 72.4, 77.2. MS (FAB+) ($m/z$): calcd for $[C_{12}H_{29}N_2O_5]^+$ 281.2, found 281.2.

*H(17O5,2)-Cbz (**4h**).* This compound was prepared by the similar procedure as described for preparing compound **4d**, except compound **3h** (0.56 g, 2 mmol) was used instead of 5LIO-amine. Separation and purification were performed as described above. Compound **4h** was obtained as a beige thick oil. Yield: 1.5 g (75% based on diamine). $^1$H NMR (300 MHz, $CDCl_3$): $\delta$ 2.61 (s, 12H), 3.19 (m, 8H), 3.44 (m, 8H), 3.48 (s, 12H), 5.05 (s, 8H), 5.79 (s, 4H), 7.29 (s, 20H). $^{13}$C NMR (300 MHz, $CDCl_3$): $\delta$ 39.0, 53.0, 54.1, 66.3, 70.0, 70.2, 70.3, 70.4, 77.2, 127.9, 128.0, 128.3, 136.7, 156.7. MS (FAB+) ($m/z$): calcd for $[C_{52}H_{72}N_6O_{13}]^+$ 989.5, found 989.5.

*H(17O5,2)-Amine (**5h**).* H(17O3,2)-Cbz (0.9 g, 1 mmol) was dissolved in 20 mL of methanol and hydrogenated at 25 °C (cooling with a water bath) and 500 psi in the presence of 10% Pd/C (0.2 g). Filtration of the catalyst and evaporation of the solvent gave 0.39 g (90%) of H(17O5,2)-amine. $^1$H NMR (400 MHz, $D_2O$): $\delta$ 2.75 (s, 4H), 2.87 (m, 8H), 3.22 (m, 8H), 3.54 (s, 4H), 3.72 (s, 16H). $^{13}$C NMR (100 MHz, $D_2O$): $\delta$ 39.0, 55.3, 58.7, 69.3, 71.3, 72.2. MS (FAB +) ($m/z$): calcd for $[C_{20}H_{49}N_6O_5]^+$ 453.3, found 453.4.

*H(17O5,2)-1,2-HOPOBn (**6h**).* This compound was prepared by the similar procedure as described for preparing compound **6d**, except compound **5h** (230 mg, 0.5 mmol) was used instead of compound **5d**. Separation and purification were performed as described above. Compound **6h** was obtained as a pale yellow thick oil. Yield: 0.48 g (72% based on the free amine). $^1$H NMR (500 MHz, $CDCl_3$) $\delta$ 2.40 (s, 4H), 2.52 (s, 8H), 3.11 (m, 4H), 3.23 (s, 20H), 3.31(m, H), 5.31 (s, 8H), 6.19 (d, $J$ = 6 Hz, 4H), 6.58 (d, $J$ = 9 Hz, 4H), 7.22 (dd, $J$ = 9.0 Hz, 4H), 7.34 (m, 12H), 7.52 (m, 12H). $^{13}$C NMR (100 MHz, $CDCl_3$): $\delta$ 37.6, 52.2, 53.2, 69.6, 69.7, 77.0, 77.4, 78.77, 104.5, 122.8, 128.0, 128.8, 129.7, 133.3, 137.9, 143.1, 158.1, 160.5. MS (FAB+) ($m/z$): calcd for $[C_{72}H_{85}N_{10}O_{17}]^+$ 1361.6, found 1361.7.

*H(17O5,2)-1,2-HOPO (**7h**).* H(17O5,2)-1,2-HOPOBn was deprotected with concentrated HCl (12 M)/glacial acetic acid (1:1) as mentioned above for preparing **7b**. An off-white foam was obtained as product. Yield: 90%. $^1$H NMR (300 MHz, $CD_3OD$): $\delta$ 3.34 (s, 8H), 3.39 (s, 4H), 3.46 (s, 16H), 3.66 (s, 8H), 3.72 (s, 4H), 6.57 (d, $J$ = 8 Hz, 8H), 7.28 (d, $J$ = 8 Hz, 4H). $^{13}$C NMR (75 MHz, $CD_3OD$): $\delta$ 36.5, 54.9, 55.1, 66.0, 71.2, 71.4, 71.5, 109.6, 121.4, 138.9, 141.1, 160.1, 163.4. Anal. Calcd for $C_{44}H_{60}N_{10}O_{17}\cdot 2HCl\cdot 5H_2O$: C, 45.40; H, 6.24; N, 12.03. Found: C, 45.09; H, 6.35; N, 11.86. MS (FAB+) ($m/z$): calcd for $[C_{44}H_{60}N_{10}O_{17}]^+$ 1001.4, found 1001.4.

*Preparation of Eu Complexes.* To a solution of ligand (0.01 mmol) in MeOH (5 mL) in a 10 mL round-bottom flask was added a solution of 1.0 equiv of $EuCl_3\cdot 6H_2O$ in MeOH (1 mL), and the mixture was stirred for 15 min; pyridine (15 $\mu$L) was then added. The mixture was heated to reflux temperature for 4 h with stirring. Upon cooling, a white solid formed which was collected by centrifuge, washed with a small amount (~3 mL) of methanol (complexes with ligands H(2,2)-1,2-HOPO, H(3,2)-1,2-HOPO, H(4,2)-1,2-HOPO, H(5O,2)-1,2-HOPO, and H(8O2,2)-1,2-HOPO) or isopropanol (complexes with ligands H(11O3,2)-1,2-HOPO, H(14O4,2)-1,2-HOPO, and H-(17O5,2)-1,2-HOPO), and air dried, yielding the desired complexes as beige powders (60−89%).

*Eu(H(3,2)-1,2-HOPO).* Yield: 60%. Anal. Calcd for $EuC_{35}H_{39}N_{10}O_{12}\cdot 2H_2O$: C, 42.91; H, 4.42; N, 14.30. Found: C, 42.73; H, 4.51. N, 14.01. HRMS-ESI ($m/z$): $[M - H]^-$ calcd for $^{151}EuC_{35}H_{38}N_{10}O_{12}$ 941.1875, found 941.1855. The observed isotopic distribution pattern matched the calculated one (Figure S1, Supporting Information).

*Eu(H(4,2)-1,2-HOPO).* Yield: 78%. Anal. Calcd for $EuC_{36}H_{41}N_{10}O_{12}\cdot H_2O$: C, 44.31; H, 4.44; N, 14.05. Found: C, 44.14; H, 4.56; N, 14.05. HRMS-ESI ($m/z$): $[M - H]^-$ calcd for $^{151}EuC_{36}H_{40}N_{10}O_{12}$ 955.2031, found 955.2021. The observed isotopic distribution pattern matched the calculated one (Figure S2, Supporting Information).

*Eu(H(5O,2)-1,2-HOPO).* Yield: 89%. Anal. Calcd for $EuC_{36}H_{41}N_{10}O_{13}\cdot 2H_2O$: C, 42.82; H, 4.49; N, 13.87. Found: C, 43.01; H, 4.67; N, 13.60. HRMS-ESI ($m/z$): $[M - H]^-$ calcd for $^{151}EuC_{36}H_{40}N_{10}O_{13}$ 971.1980, found 971.1987. The observed isotopic distribution pattern matched the calculated one (Figure S3, Supporting Information).

*Eu(H(8O2,2)-1,2-HOPO).* Yield: 70%. Anal. Calcd for $EuC_{38}H_{45}N_{10}O_{14}\cdot 5H_2O$: C, 41.20; H, 5.00; N, 12.64. Found: C, 41.13; H, 5.05; N, 12.50. HRMS-ESI ($m/z$): $[M - H]^-$ calcd for $^{151}EuC_{38}H_{44}N_{10}O_{14}$ 1015.2243, found 1015.2231. The observed isotopic distribution pattern matched the calculated one (Figure S4, Supporting Information).

*Eu(H(11O3,2)-1,2-HOPO).* Yield: 73%. Anal. Calcd for $EuC_{40}H_{49}N_{10}O_{15}\cdot 6H_2O$: C, 41.07; H, 5.26; N, 11.97. Found: C, 41.34; H, 5.01; N, 11.71. HRMS-ESI ($m/z$): $[M - H]^-$ calcd for $^{151}EuC_{40}H_{48}N_{10}O_{15}$ 1059.2505, found 1059.2481. The observed isotopic distribution pattern matched the calculated one (Figure S5, Supporting Information).

*Eu(H(14O4,2)-1,2-HOPO).* Yield: 63%. Anal. Calcd for $EuC_{42}H_{53}N_{10}O_{16}\cdot 5H_2O$: C, 42.18; H, 5.31; N, 11.71. Found: C, 42.03; H, 5.06; N, 11.55. HRMS-ESI ($m/z$): $[M - H]^-$ calcd for $^{151}EuC_{42}H_{52}N_{10}O_{16}$ 1103.2767, found 1103.2740. The observed isotopic distribution pattern matched the calculated one (Figure S6, Supporting Information).

*Eu(H(17O5,2)-1,2-HOPO).* Yield: 58%. Anal. Calcd for $EuC_{44}H_{57}N_{10}O_{17}\cdot 6H_2O$: C, 42.01; H, 5.53; N, 11.13. Found: C, 41.84; H, 4.94; N, 10.87. HRMS-ESI ($m/z$): $[M - H]^-$ calcd for $^{151}EuC_{44}H_{56}N_{10}O_{17}$ 1147.3023, found 1147.3003. The observed isotopic distribution pattern matched the calculated one (Figure S7, Supporting Information).

**Optical Spectroscopy.** UV−vis absorption spectra were recorded on a Varian Cary 300 double-beam absorption spectrometer. Emission spectra were acquired with a HORIBA Jobin Yvon IBH FluoroLog-3 spectrofluorimeter, equipped with 3-slit double-grating excitation and emission monochromators (2.1 nm/mm dispersion, 1200 grooves/mm). Spectra were reference corrected for both the excitation light source variation (lamp and grating) and the emission spectral response (detector and grating). Luminescence lifetimes were determined on the same HORIBA Jobin Yvon IBH FluoroLog-3 spectrofluorimeter, adapted for time-correlated single-photon counting (TCSPC) and multichannel scaling (MCS) measurements. A submicrosecond Xenon flashlamp (Jobin Yvon, 5000XeF) was used as the light source, with an input pulse energy (100 nF discharge capacitance) of ca. 50 mJ, yielding an optical pulse duration of less than 300 ns at fwhm. Spectral selection was achieved by passage through the same double-grating excitation monochromator. Emission was monitored perpendicular to the excitation pulse, again with spectral selection achieved by passage through the double-grating emission monochromator (2.1 nm/mm dispersion, 1200 grooves/mm). A thermoelectrically cooled single-photon detection module (HORIBA Jobin Yvon IBH, TBX-04-D) incorporating fast rise time PMT, wide bandwidth preamplifier and picosecond constant fraction discriminator was used as the detector. Signals were acquired using an IBH DataStation Hub photon counting module, and data analysis was performed using the commercially available DAS 6 decay analysis software package from HORIBA Jobin


DOI: 10.1021/acs.inorgchem.5b00748
*Inorg. Chem.* 2015, 54, 6807−6820

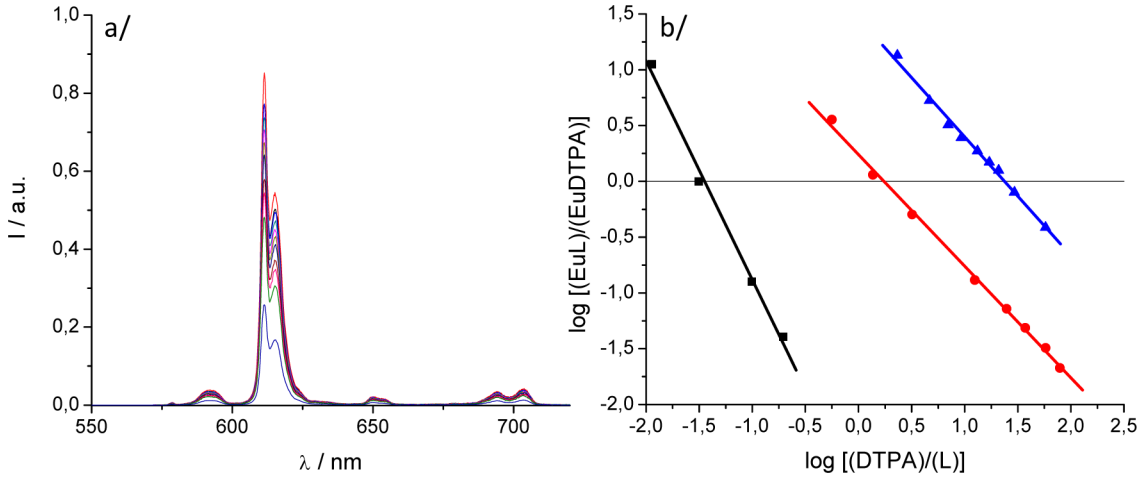


**Figure 1.** (a) Luminescence spectrum showing the typical decrease of luminescence intensity upon addition of increasing amounts of DTPA; (b) DTPA competition batch titration of $[Eu(H(3,2)\text{-}1,2\text{-}HOPO)]^-$ (black squares, line), $[Eu(H(5O,2)\text{-}1,2\text{-}HOPO)]^-$ (red circles, line), and $[Eu(H(11O3,2)\text{-}1,2\text{-}HOPO)]^-$ (blue triangles, line) versus DTPA. The *x* intercept indicates the difference in pEu between EuDTPA (pEu = 19.04) and the two complexes.

**Chart 1. Chemical Structures of the Tetradentate Model Compound 5LIN$^{Me}$-1,2-HOPO (left) and the Octadentate 1,2-HOPO Ligands Investigated (center, right)**

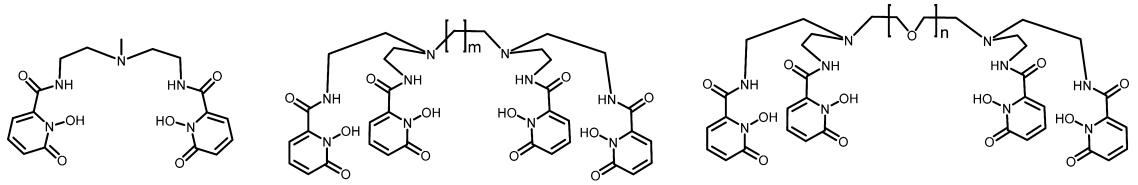

5LIN$^{Me}$-1,2-HOPO

m=1, H(2,2)-1,2-HOPO
m=2, H(3,2)-1,2-HOPO
m=3, H(4,2)-1,2-HOPO

n=1, H(5O,2)-1,2-HOPO
n=2, H(8O2,2)-1,2-HOPO
n=3, H(11O3,2)-1,2-HOPO
n=4, H(14O4,2)-1,2-HOPO
n=5, H(17O5,2)-1,2-HOPO

Yvon IBH. Goodness of fit was assessed by minimizing the reduced chi squared function, $\chi^2$, and a visual inspection of the weighted residuals. Each trace contained at least 10 000 points, and the reported lifetime values resulted from at least three independent measurements. Typical sample concentrations for both absorption and fluorescence measurements were ca. $10^{-5}$–$10^{-6}$ M, and 1.0 cm cells in quartz Suprasil or equivalent were used for all measurements. Quantum yields were determined by the optically dilute method (with optical density < 0.1) using the following equation

$$\Phi_x/\Phi_r = [A_r(\lambda_r)/A_x(\lambda_x)][I(\lambda_r)/I(\lambda_x)][n_x^2/n_r^2][D_x/D_r]$$

where $A$ is the absorbance at the excitation wavelength ($\lambda$), $I$ is the intensity of the excitation light at the same wavelength, $n$ is the refractive index, and $D$ is the integrated luminescence intensity. The subscripts $x$ and $r$ refer to the sample and reference, respectively. For quantum yield calculations, an excitation wavelength of 340 nm was utilized for both the reference and the sample; hence, the $I(\lambda_r)/I(\lambda_x)$ term is removed. Similarly, the refractive indices term, $n_x^2/n_r^2$, was taken to be identical for the aqueous reference and sample solutions. Hence, a plot of integrated emission intensity (i.e., $ID_r$) vs absorbance at 340 nm (i.e., $A_r$) yields a linear plot with a slope which can be equated to the reference quantum yield $\Phi_r$. Quinine sulfate in 0.5 M (1.0 *N*) sulfuric acid was used as the reference ($\Phi_r$ = 0.546).[30] By analogy, for the sample, a plot of integrated emission intensity (i.e., $D_x$) versus absorbance at 340 nm (i.e., $A_x$) yields a linear plot, and $\Phi_x$ can then be evaluated. The values reported in the manuscript are the average of four independent measurements.

For the lifetime dilution and time-dependent measurements, the samples were initially dissolved in DMSO to give a concentration of 1 mM and then diluted into TRIS buffered saline (20 mM TRIS, 100 mM NaCl, pH 7.4) to the desired final concentrations of $10^{-5}$, $10^{-6}$, and $10^{-8}$ M. An excitation wavelength of 340 nm was used, and emission lifetimes were monitored at 612 nm. Samples were analyzed immediately after dilution into buffer and then again after several different time intervals.

**Competition Batch Titrations for pEu and pZn Determination.** The general procedure used to determine the pEu values of the ligands was adapted from an already described study using Gd[31,32] and are similar to those already reported for other complexes.[29] Different volumes of a standardized DTPA stock solution were added to solutions of constant ligand, metal, and electrolyte concentrations. In the current work, the pH of all solutions was kept constant at 7.4 with TRIS buffer instead of adjusting the pH to 6.0 as was done in past studies,[31] and the solutions were diluted to identical volumes. After stirring the solutions for 24 h to ensure thermodynamic equilibrium was reached, the pH was again checked just before analyzing the samples spectrophotometrically. The concentrations of each ligand relative to DTPA used in the final data analysis ranged from 1:1 to 1:1000 (L:DTPA). Concentrations of free and complexed ligand in each solution were determined from the luminescence spectra at identical pH and concentrations. These concentrations were used for the log/log plots (Figure 1) to give the difference in pEu between the competing DTPA and ligand of interest. In a similar way, pZn was determined by using a solution of $ZnCl_2$ in water as a competitor instead of DTPA.

## RESULTS AND DISCUSSION

**Design of the Ligands and Synthesis.** The tetradentate ligand 5LIN$^{Me}$-1,2-HOPO was prepared as described elsewhere,[29] and all octadentate ligands were prepared in a similar way to the previously reported H(2,2)-1,2-HOPO ligand. Since



DOI: 10.1021/acs.inorgchem.5b00748
*Inorg. Chem.* 2015, 54, 6807–6820

the complex ([Eu(H(2,2)-1,2-HOPO)]$^-$) has been shown to have one water molecule in its inner sphere,[29] which limits its overall quantum yield, the central ethyl chain was substituted by longer aliphatic chains (propyl and butyl) or polyethylene glycol (PEG) chains yielding a more flexible ligand backbone for the two essentially "5LIN$^{Me}$-1,2-HOPO-like" motifs to bind in a similar way to the model bis-tetradentate [Eu(5LIN$^{Me}$-1,2-HOPO)$_2$]$^-$ complex, in order to achieve enhanced optical properties, vide infra. Noticeably, the addition of the PEG groups is also expected to increase the solubility of the ligand, and this alteration has proven successful in increasing the solubility of luminescent lanthanide complexes.[23,33,34] For these ligands, we adopted the H(XOn,Y) notation, where the X index refers to the total number of atoms in the central chain between the two bridgehead tertiary nitrogen atoms which connect each pair of terminal 1,2-HOPO units, and the Y index refers to the number of atoms between the bridgehead tertiary nitrogen atom and the N atom of the 1,2-HOPO amide linkage. Additional nomenclature after the X refers to the number ($n$) of ether oxygen atoms (O) in the central chain. For example, for H(11O3,2), there are two carbons atoms between the 1,2-HOPO amide and the bridgehead tertiary nitrogen atoms, while the central chain contains a total of 11 atoms, of which three are oxygen atoms (see Chart1).

The syntheses of the H($m$,2)-1,2-HOPO ligands were straightforward (Scheme 1). The backbone amines of H(3,2)-1,2-HOPO and H(4,2)-1,2-HOPO, *N,N,N′,N′*-tetrakis(2-aminoethyl)-propane-1,2-diamine, and *N,N,N′,N′*-tetrakis(2-amino-ethyl)-butane-1,4-diamine were prepared as reported elsewhere.[35]

The H($m$On,2)-1,2-HOPO ligands were synthesized from the corresponding $\alpha,\omega$-glycol-diamine (Scheme 2). While 2-(2-amino-ethoxy)-ethylamine (5LIO-diamine) (**3d**) and 2-[2-(2-amino-ethoxy)-ethoxy]-ethylamine (**3e**) are commercially available, other oligoethylene glycol diamines (**3f−h**) were prepared from the corresponding oligoethylene glycols as shown in Scheme 2. The oligoethylene glycols were converted to corresponding mesylates (**1f−h**), which were transformed into the diazides (**2f−h**) by reaction with sodium azide. The diamines (**3f−h**) were prepared from the diazides (**2f−h**) by catalytic hydrogenation over Pd/C. The protected H($m$On,2)-tetraamines (**4d−h**) were synthesized by the reaction of the appropriate oligoethylene glycol diamines (**3d−h**) with benzyl aziridine-1-carboxylate, with subsequent deprotection of the Cbz group by hydrogenation giving H($m$On,2)-tetraamines in good yields. Amide coupling of the H($m$On,2)-tetraamines with 1,2-HOPOBn-thiazolide or 1,2-HOPOBn acid chloride[36,37] yields the benzyl-protected ligands (**6d−h**), which were deprotected under acidic conditions with 1:1 (v/v) AcOH/HCl (12 M) to yield the target 1,2-HOPO ligands (**7d−h**).

The Eu(III) complexes were prepared by refluxing equal equivalents of the appropriate ligand with $EuCl_3{\cdot}6H_2O$ in methanol using pyridine as a base to ensure complete complexation. The desired complexes were then precipitated, isolated by centrifuging, and washed with either methanol or isopropanol to yield analytically pure hydrated complexes. Since the same results were obtained by mixing equal equivalents of the ligand with $EuCl_3{\cdot}6H_2O$ (and allowing to equilibrate overnight), the Gd(III) complexes were prepared in situ using the latter method. The full characterization of the ligands and isolated complexes and synthetic details are reported in the Experimental Section.

**Thermodynamic Stability.** One practical concern related to the use of europium chelators for biological applications is the thermodynamic stability of the complexes. It should also be noted that the kinetic inertness of the corresponding complexes is similarly a very important factor to consider for biological applications.[3,38,39] In biological media, many factors can influence the stability of the metal complex, such as the competition of proton, endogenous cations (e.g., $Ca^{2+}$, $Zn^{2+}$, $Mg^{2+}$) and anions (hydroxide, phosphate), and also natural chelators such as transferrin or albumin. In order to determine their thermodynamic stabilities, spectrophotometric titration studies were performed in terms of the pEu value for all 1,2-HOPO derivatives. Analogous to pH, pEu is defined as the negative log of the concentration of free metal in solution (pEu= $-\log [Eu^{3+}]_{free}$) at a specified set of standard conditions (typically $[Eu]_T$ = 1 $\mu$M, $[L]_T$ = 10 $\mu$M, pH = 7.4, 25 °C, and 0.1 M KCl). The evaluated pEu values therefore offer a convenient way to compare relative chelate thermodynamic stabilities between various ligands, regardless of their differing protonation behavior.

The method chosen to determine this conditional thermodynamic stability parameter was competition batch titration using the potent octadentate chelator, diethylenetriamine pentaacetic acid (DTPA) as the competing ligand which is widely used in industry. The FDA has approved $CaNa_3$-DTPA injection and $ZnNa_3$DTPA injection for treatment of individuals with known or suspected internal contamination with plutonium, americium, or curium to increase the rates of elimination (www.fda.gov/drugs/EmergencyPreparedness/).

In this experiment, the concentrations of ligands and Eu(III) as well as the pH were kept constant while the concentration of DTPA was progressively increased. Figure 1a shows the luminescence spectra obtained for one of the complexes and the evolution upon addition of varying amounts of DTPA. From the luminescence data, the resulting concentrations of free and complexed ligand were determined, and a plot of $\log([EuL]^-/[EuDTPA]^{2-})$ vs $\log([DTPA]/[L])$ was constructed (Figure 1b), which directly yields the difference in pEu between the studied ligands and DTPA (i.e., from the $x$ axis intercept, $\Delta$pEu = $\log([DTPA]/[L]$ when $\log([EuL]^-/[EuDTPA]^{2-}$ = 0, or, alternately, this is the concentration of DTPA which generates equal partition of Eu between the described ligands and DTPA). Using the known pEu of 19.04 for DTPA,[40] the pEu of all Eu(III) complexes were calculated using luminescence spectroscopy.

The stability values in terms of pEu (see Table 1) vary slightly from one ligand to the other spanning from 19.9 to 21.2

**Table 1. Thermodynamic Parameters Related with the Stability of The Eu(III) and Zn(II) Complexes with the Discussed Ligands in TRIS Buffered Solution (pH = 7.4)**

| | pEu | pZn |
|---|---|---|
| H(2,2)-1,2-HOPO[29] | 21.2(1) | 17.2(4) |
| H(3,2)-1,2-HOPO | 17.5(1) | 13.7(5) |
| H(4,2)-1,2-HOPO | 18.4(2) | 14.7(4) |
| H(5O,2)-1,2-HOPO | 19.2(1) | 15.6(4) |
| H(8O2,2)-1,2-HOPO | 20.4(1) | 16.9(4) |
| H(11O3,2)-1,2-HOPO | 20.4(1) | 17.4(3) |
| H(14O4,2)-1,2-HOPO | 20.3(1) | 16.9(4) |
| H(17O5,2)-1,2-HOPO | 20.0(1) | 16.8(3) |
| 5LIN$^{Me}$-1,2-HOPO[29] | 17.3(1) | 14.8(4) |



DOI: 10.1021/acs.inorgchem.5b00748
*Inorg. Chem.* 2015, 54, 6807−6820

for most of the octadentate ligands except for [Eu(H(3,2)-1,2-HOPO)]$^-$ and [Eu(H(4,2)-1,2-HOPO)]$^-$ (pEu = 17.5 and 18.4, respectively). These values establish that highly stable europium complexes are formed with thermodynamic stabilities slightly to moderately higher than that of DTPA. Most of the octadentate complexes possess pEu's higher than the bis-tetradentate model ([Eu(5LIN$^{Me}$-1,2-HOPO)$_2$]$^-$ (pEu = 17.3), which can be attributed to the enhanced chelate effect arising from an octadentate versus bis-tetradentate topology, in addition to increased ligand preorganization. Interestingly, [Eu(H(2,2)-1,2-HOPO)]$^-$ is the most thermodynamically stable complex within this series (pEu = 21.2). This result is somewhat surprising since the backbone of all the complexes is similar but can be rationalized presumably by an essentially ideal nonacoordinated geometry of the ensuing complex (where the ninth site is occupied by one water molecule as shown elsewhere[29]) and the existence of intramolecular H-bonding interactions between the tertiary amines previously noted elsewhere[34] which stabilizes the Eu(III) complex. For [Eu(H(3,2)-1,2-HOPO)]$^-$, [Eu(H(4,2)-1,2-HOPO)]$^-$, and [Eu(H(5O,2)-1,2-HOPO)]$^-$, the smaller pEu values suggest that the complexation geometry is slightly different with complexes slightly more constrained compared to [Eu(H-(8O2,2)-1,2-HOPO)]$^-$, [Eu(H(11O3,2)-1,2-HOPO)]$^-$, [Eu-(H(14O4,2)-1,2-HOPO)]$^-$, and [Eu(H(17O4,2)-1,2-HOPO)]$^-$. All of the latter complexes, with long central chains, possess pEu values around ca. 20, which are one order of magnitude lower than [Eu(H(2,2)-1,2-HOPO)]$^-$ but one order higher than the benchmark DTPA. Such impressive aqueous stability allows measurements to be performed at submicromolar concentration without observable decomposition of the complexes.

Notably, for the longer chain backbones, we also considered the possibility of bimetallic dimeric [Eu$_2$L$_2$]$^{2-}$ complex formation. Although the pEu's determined in this manner cannot differentiate between [ML]$^-$ and [M$_2$L$_2$]$^{2-}$ complexes, the single-exponential decay behavior we observe suggests only a single emitting species in solution, which based on thermodynamic grounds should be the monomeric EuL complex. Furthermore, we conducted additional luminescence lifetime experiments upon serial dilution of the [Eu(H(8O2,2)-1,2-HOPO)]$^-$, [Eu(H(11O3,2)-1,2-HOPO)]$^-$, [Eu(H-(14O4,2)-1,2-HOPO)]$^-$, and [Eu(H(17O5,2)-1,2-HOPO)]$^-$ complexes at three different concentrations representing the range of concentrations used for quantum yield measurements ($10^{-5}$ and $10^{-6}$ M) and also at nanomolar concentration (10 nM). At very low concentrations, any potentially dimeric [Eu$_2$L$_2$]$^{2-}$ complexes (or polymeric [Eu$_n$L$_n$]$^{n-}$ species) would be thermodynamically disfavored due to their second-order (or higher) concentration dependence. However, the observed luminescence lifetimes obtained immediately after dilution and again after several different time intervals (10 min, 1 h, 4 days) remained unchanged within experimental error, with all complexes exhibiting monoexponential decays, providing additional evidence that the complex observed in solution is indeed the monomeric [ML]$^-$ species.

To ensure that the thermodynamic stability of the complexes is high enough for biological measurements, their stability vs slightly basic or acidic conditions or vs Ca(II) or Zn(II) was also estimated. As can be seen from Figure S8, Supporting Information, the 1,2-HOPO moiety is highly stable to basic or acidic conditions (TRIS solution at pH = 6.1, 7.4, 8.5), yielding no change in emission intensity over days when measured at 612 nm using the intense $J$ = 2 transition. This high stability is due to the rather low p$K_a$ (~5) of the 1,2-HOPO moieties.[41]

Similarly, no decomposition of the complexes was observed when measurements were performed in 20 mM $CaCl_2$ solution, revealing the absence of affinity of 1,2-HOPO ligands for this metal cation (Figure S9, Supporting Information).

However, in the presence of Zn(II), at 20 mM in TRIS buffer (pH = 7.4), a total loss of the Eu(III) luminescence was observed. As a consequence, the stability of the Eu(III) complex versus the Zn(II) ion was measured in terms of the pZn. These pZn were measured in an analogous way to the described DTPA batch titration, substituting DTPA by a solution with a known concentration of $ZnCl_2$.

As seen in Table 1, the pZn values are all much lower (by 3 to 4 orders of magnitude) than the pEu, demonstrating the weaker interaction of the 1,2-HOPO ligands with Zn(II) and therefore the specificity of such ligands to preferentially bind the Eu(III) cation in biological media where the free Zn(II) concentration is comparably low. It is interesting to note that the same trend of the Eu(III) ions is followed with the Zn(II) ion (Figure S10, Supporting Information).

**UV−Vis Absorption Spectroscopy.** The UV−vis absorption data for each of the Eu(III) complexes in TRIS buffer solution (pH = 7.4) are summarized in Table 2. Each of the spectra have absorption maximal around 335−340 nm (Figure 2). Those bands are composed of two electronic transitions; at higher energy, a purely $\pi-\pi^*$ transition and at slightly lower energy (ca. 320 nm) a $\pi-\pi^*$ transition with some n$-\pi^*$ character, as evidenced previously from TD-DFT calculations.[9,42] Absorption maxima are slightly shifted toward higher energy upon increasing the bridge length, and this has previously been proposed to be due to a small interaction between the terminal 5LIN$^{Me}$-1,2-HOPO units.[29] This interaction gives maxima blue shifting from 341 nm for [Eu(H(2,2)-1,2-HOPO)]$^-$ to 334 nm for [Eu(H(17O5,2)-1,2-

**Table 2. UV−Vis Absorption Data of the Studied Eu(III) Complexes in TRIS Buffer (pH = 7.4); Brightness at Maximum Absorption and Triplet Excited State Energies**

| | TRIS buffer pH = 7.4 | | | |
|---|---|---|---|---|
| | $\lambda_{abs}^{max}$ (nm) | $\varepsilon$ ($M^{-1}\cdot cm^{-1}$) | brightness ($M^{-1}\cdot cm^{-1}$) | 77 K,[a] $T_{0-0}$/ nm ($cm^{-1}$) |
| [Eu(H(2,2)-1,2-HOPO)]$^-$ [29] | 341 | 18 200 | 655 | 21 980 |
| [Eu(H(3,2)-1,2-HOPO)]$^-$ | 339 | 17 700 | 655 | 21 900 |
| [Eu(H(4,2)-1,2-HOPO)]$^-$ | 337 | 17 900 | 555 | 22 390 |
| [Eu(H(5O,2)-1,2-HOPO)]$^-$ | 337 | 15 900 | 1065 | 22 000 |
| [Eu(H(8O2,2)-1,2-HOPO)]$^-$ | 336 | 15 350 | 1720 | 22 320 |
| [Eu(H(11O3,2)-1,2-HOPO)]$^-$ | 334 | 15 070 | 2485 | 22 120 |
| [Eu(H(14O4,2)-1,2-HOPO)]$^-$ | 336 | 15 200 | 2920 | 22 020 |
| [Eu(H(17O5,2)-1,2-HOPO)]$^-$ | 336 | 15 000 | 2940 | 21 690 |
| [Eu(5LIN$^{Me}$-1,2-HOPO)$_2$]$^-$ [29] | 332 | 18 050 | 3120 | 22 010 |

[a]Determined in a solid matrix at 77 K (methanol:ethanol, 1:4 v/v) using the Gd complexes. Estimated error in $\varepsilon$ and brightness ($\varepsilon \times \phi_{Tot}$) are 15% and 20%, respectively



DOI: 10.1021/acs.inorgchem.5b00748
Inorg. Chem. 2015, 54, 6807−6820

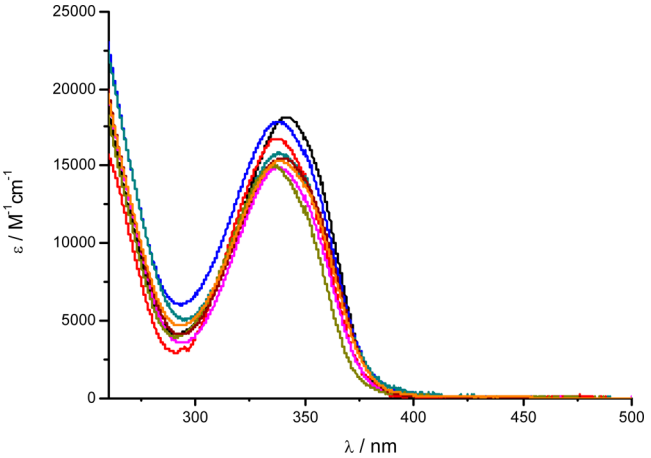


**Figure 2.** UV−vis absorption spectra of [Eu(H(2,2)-1,2-HOPO)]$^-$ (black), [Eu(H(3,2)-1,2-HOPO)]$^-$ (red), Eu(H(4,2)-1,2-HOPO)]$^-$ (blue), [Eu(H(5O,2)-1,2-HOPO)]$^-$ (aqua), [Eu(H(8O2,2)-1,2-HOPO)]$^-$ (magenta), [Eu(H(11O3,2)-1,2-HOPO)]$^-$ (olive), Eu-(H(14O4,2)-1,2-HOPO)]$^-$ (orange), and [Eu(H(17O5,2)-1,2-HOPO)]$^-$ (dark red) in 0.1 M TRIS buffer (pH = 7.4).

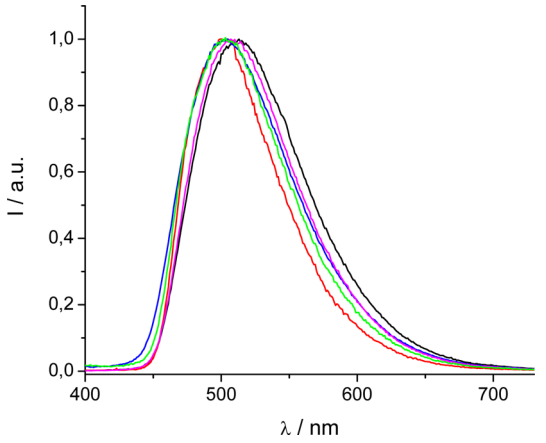


**Figure 3.** Time-gated phosphorescence spectra of [Gd(H(2,2)-1,2-HOPO)]$^-$ (black), [Gd(H(3,2)-1,2-HOPO)]$^-$ (red), [Gd(H(4,2)-1,2-HOPO)]$^-$ (blue), [Gd(H(5O,2)-1,2-HOPO)]$^-$ (magenta), and [Gd(H(11O3,2)-1,2-HOPO)]$^-$ (green) in methanol:ethanol (1:4 v/v) at 77 K ($\lambda_{ex}$ = 330 nm, delay 0.1 ms).

HOPO)]$^-$ (as low as 332 nm for the previously reported [Eu(5LIN$^{Me}$-1,2-HOPO)$_2$]$^-$ complex). At the same time, the molar absorption coefficients decrease considerably as the length of the central bridge is increased, by as much as 15% for [Eu(H(17O5,2)-1,2-HOPO)]$^-$ compared to other 1,2-HOPO complexes previously reported.[9,29,43]

It should be noticed that no differences were observed when comparing the UV−vis absorption spectra of the gadolinium and europium complexes. Furthermore, inspection of the UV−vis properties of the free ligand under the same conditions reveals the same blue shift of the absorption maximum upon increasing the length of the central bridge. This result reveals that the effect observed with europium (and gadolinium) arises from an interaction between the terminal 5LIN$^{Me}$-1,2-HOPO motifs within one octadentate ligand.

**Luminescence of Gd Complexes.** Estimation of the energies of the ligand-based triplet excited state were determined using the Gd(III) complexes. Gadolinium was chosen since it is a 4f $^7$ lanthanide cation having a similar electronic configuration and size as the europium cation (4f $^6$) but lacking any accessible metal-based low-energy electronic excited states. At room temperature, only a broad weak emission centered between 380 and 400 nm can be seen for the Gd(III) complexes, which can be attributed to the poorly emissive singlet excited state of the 1,2-HOPO chromophore in complex with the gadolinium cation.[9,42] At 77 K, in a 1:4 (v/v) methanol:ethanol solid matrix, a broad emission band at ca. 500 nm is observed (Figure 3). This emission, red shifted compared to the singlet excited state, can be assigned to phosphorescence from the triplet excited state, which is lower in energy than the singlet excited state observed at room temperature. Selective time-gated phosphorescence spectra (delay 0.1 ms) of the gadolinium complexes at 77 K are depicted in Figure 3, and the energies associated with these triplet excited states are reported in Table 2. From these values, it appears the lowest energy triplet excited state of the complexes all have approximately the same energy (22 050 ± 210 cm$^{-1}$) with a very small (<1%) standard deviation. This result suggests that the small interaction observed for the singlet excited state is absent (or weak enough to not be observed). Such small differences in the triplet excited state energies should not provide any large difference in the sensitization efficiency between complexes, since all triplet excited states possess almost the same energy gap with respect to the $^5$D$_2$ (E = 21 519 cm$^{-1}$) and the $^5$D$_1$ (E = 19 028 cm$^{-1}$) accepting levels of europium.

**Luminescence of Eu Complexes.** As expected from the difference in crystal field, the nonacoordinated and octacoordinated complexes present some significant differences in their luminescence pattern, with different relative intensities and splitting for all transitions (see Figure 4) giving an unusual type of spectrum for [Eu(H(2,2)-1,2-HOPO)]$^-$ compared to all 1,2-HOPO octacoordinated derivatives. For all octacoordinated complexes, as can be seen in Figure 4, the emission spectra are typical with very intense $J$ = 2 transitions ($^5$D$_0$ → $^7$F$_2$). The intensity of the $J$ = 1 band ($^5$D$_0$ → $^7$F$_1$) changes as compared to the overall intensity (Figure 4), yielding different luminescence radiative parameters (vide infra).[44,45] Also, the splitting pattern of the $J$ = 1 transition changes, which clearly indicates a change in the geometry around the metal center. Of interest is also the similarities in pattern and spectra of [Eu(H(2,2)-1,2-HOPO)]$^-$ and [Eu(H(3,2)-1,2-HOPO)]$^-$, with intense $J$ = 1 and 4 bands (when compared to the $J$ = 2), suggesting that the emission observed for [Eu(H(3,2)-1,2-HOPO)]$^-$ may also arise from a nonacoordinated species (as previously observed for [Eu(H-(2,2)-1,2-HOPO)]$^-$).[29] For [Eu(H(4,2)-1,2-HOPO)]$^-$, as shown in Figure 5, we note that the $J$ = 4 transition is intermediate between [Eu(H(2,2)-1,2-HOPO)]$^-$ and [Eu(H-(5O,2)-1,2-HOPO)]$^-$ (as an example of all other complexes with longer bridges), suggesting the presence of two different emitting species in solution (one nona- and the other octacoordinated). This change in pattern is also observed at 77 K, in solid matrix, supporting the change of geometry around the Eu(III) ion (see Figure 5b). Importantly, the position of the $J$ = 0 transitions is unique for all differing emitting complexes in solution, but the broadness of this transition in this case (even at 77 K) precludes any definitive conclusion. As shown in Figure 5b, the $^5$D$_0$ → $^7$F$_1$ transition is composed of three peaks for all europium(III) complexes at room temperature and at 77 K in solid matrix. While the broadness of the transition again precludes a definitive determination of the exact point group of the complex, such multiplicity suggests that from the three most common


DOI: 10.1021/acs.inorgchem.5b00748
*Inorg. Chem.* 2015, 54, 6807−6820

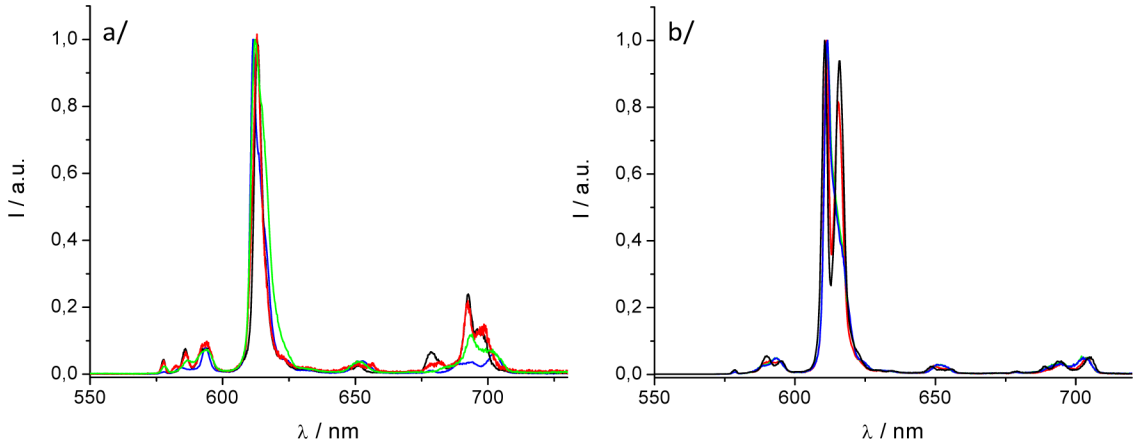


**Figure 4.** (a) Luminescence spectra of [Eu(H(2,2)-1,2-HOPO)]$^-$ (black), [Eu(H(3,2)-1,2-HOPO)]$^-$ (red), [Eu(H(4,2)-1,2-HOPO)]$^-$ (green), and [Eu(H(5O,2)-1,2-HOPO)]$^-$ (blue) and (b) [Eu(H(8O2,2)-1,2-HOPO)]$^-$ (black), [Eu(H(11O3,2)-1,2-HOPO)]$^-$ (red), [Eu(H(14O4,2)-1,2-HOPO)]$^-$ (green), and [Eu(H(17O5,2)-1,2-HOPO)]$^-$ (blue) at room temperature in 0.1 M TRIS buffer at pH = 7.4 ($\lambda_{ex}$ = 340 nm).

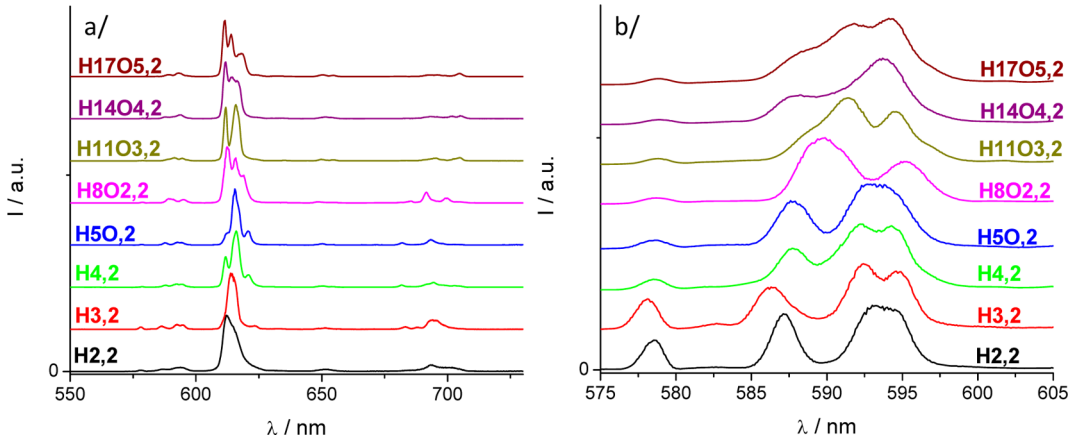


**Figure 5.** Luminescence spectra and highlight of the $J$ = 0 and 1 transitions of [Eu(H(2,2)-1,2-HOPO)]$^-$ (black), [Eu(H(3,2)-1,2-HOPO)]$^-$ (red), [Eu(H(4,2)-1,2-HOPO)]$^-$ (green), and [Eu(H(5O,2)-1,2-HOPO)]$^-$ (blue) and [Eu(H(8O2,2)-1,2-HOPO)]$^-$ (magenta), [Eu(H(11O3,2)-1,2-HOPO)]$^-$ (olive), [Eu(H(14O4,2)-1,2-HOPO)]$^-$ (purple), and [Eu(H(17O5,2)-1,2-HOPO)]$^-$ (dark red) at 77 K in solid matrix (ethanol:methanol 4:1) ($\lambda_{ex}$= 340 nm).

coordination polyhedra, the best match to the observed luminescence spectra is obtained for the bicapped trigonal prism ($C_{2v}$) geometry as noted elsewhere for similar derivatives.[46]

In addition to the steady state emission spectra, the luminescence quantum yields and luminescence lifetimes of the Eu(III) complexes were also measured in aqueous solution with 0.1 M TRIS buffer pH = 7.4 and in deuterated solution to estimate the number of inner-sphere water molecules (i.e., $q$) using the improved Horrock's equation.[47] All photophysical characterizations are summarized in Table 3.

As can be readily seen, the central bridge influences all the luminescence properties by inducing constraint on the complexation geometry for shorter bridges. Increasing the chain length results in a subsequent increase of the luminescence efficiency, going from 0.031 to 0.196 for [Eu(H(4,2)-1,2-HOPO)]$^-$ and [Eu(H(17O5,2)-1,2-HOPO)]$^-$, respectively (see also Figure 8a). In more detail, the luminescence quantum yields are in the same order from [Eu(H(2,2)-1,2-HOPO)]$^-$ to [Eu(H(4,2)-1,2-HOPO)]$^-$; then a constant increase is observed until reaching a plateau for [Eu(H(14O4,2)-1,2-HOPO)]$^-$ and [Eu(H(17O5,2)-1,2-HOPO)]$^-$ (Figure 8a). Noticeably, the maximum quantum

**Table 3. Photophysical Data of the Investigated Eu Complexes**

| | 0.1 M TRIS buffer pH = 7.4 | | | | 77 K[a] |
|---|---|---|---|---|---|
| | $\phi_{Tot}$ | $\tau$ ($\mu$s) | $\tau^D$ ($\mu$s) | $q$ | $\tau$ ($\mu$s) |
| [Eu(H(2,2)-1,2-HOPO)]$^-$ [29] | 0.036 | 480 | 1222 | 1.1 | 914 |
| [Eu(H(3,2)-1,2-HOPO)]$^-$ | 0.037 | 552; 253 | 811; 369 | 0.3; 1.0 | 1040; 781 |
| [Eu(H(4,2)-1,2-HOPO)]$^-$ | 0.031 | 649; 236 | 803; 338 | 0; 1.1 | 902; 645 |
| [Eu(H(5O,2)-1,2-HOPO)]$^-$ | 0.067 | 651; 304 | 825; 462 | 0; 1.1 | 823; 608 |
| [Eu(H(8O2,2)-1,2-HOPO)]$^-$ | 0.112 | 697 | 913 | 0 | 748 |
| [Eu(H(11O3,2)-1,2-HOPO)]$^-$ | 0.165 | 668 | 888 | 0.1 | 765 |
| [Eu(H(14O4,2)-1,2-HOPO)]$^-$ | 0.192 | 700 | 961 | 0.1 | 819 |
| [Eu(H(17O5,2)-1,2-HOPO)]$^-$ | 0.196 | 704 | 962 | 0.1 | 826 |
| [Eu(5LIN$^{Me}$-1,2-HOPO)$_2$]$^-$ [29] | 0.173 | 728 | 1000 | 0.1 | 860 |

[a]Measured in a solid matrix at 77 K (methanol:ethanol 1:4 v/v). Estimated error in $\phi_{Tot}$ and $\tau$ are 15% and 10%, respectively



DOI: 10.1021/acs.inorgchem.5b00748
Inorg. Chem. 2015, 54, 6807−6820

yield obtained is higher than that of the model bis-tetradentate complex ($[Eu(5LIN^{Me}\text{-}1,2\text{-}HOPO)_2]^-$), suggesting that the geometry of the complexed ligand is different in octadentate structures versus bis-tetradentate structures.

As demonstrated elsewhere, the luminescence lifetime of $[Eu(H(2,2)\text{-}1,2\text{-}HOPO)]^-$ is short because of a single water molecule in its inner sphere ($\tau$ = 480 $\mu$s).[29] For the shorter central bridges, from $[Eu(H(3,2)\text{-}1,2\text{-}HOPO)]^-$ to $[Eu(H(5O,2)\text{-}1,2\text{-}HOPO)]^-$, the luminescence decay traces (Figure S11, Supporting Information) only gave satisfactory fits when modeled as biexponential decays, composed of both a short component ($\tau$ = 253, 236, and 304 $\mu$s for $[Eu(H(3,2)\text{-}1,2\text{-}HOPO)]^-$, $[Eu(H(4,2)\text{-}1,2\text{-}HOPO)]^-$, and $[Eu(H(5O,2)\text{-}1,2\text{-}HOPO)]^-$, respectively) and a longer component ($\tau$ = 552, 649, and 651 $\mu$s for $[Eu(H(3,2)\text{-}1,2\text{-}HOPO)]^-$, $[Eu(H(4,2)\text{-}1,2\text{-}HOPO)]^-$, and $[Eu(H(5O,2)\text{-}1,2\text{-}HOPO)]^-$, respectively). This biexponential luminescence decay behavior emphasizes the presence of two different species in solution with these shorter bridges. From $[Eu(H(8O2,2)\text{-}1,2\text{-}HOPO)]^-$ to $[Eu(H(17O5,2)\text{-}1,2\text{-}HOPO)]^-$, the measured luminescence lifetimes are all monoexponential and in the same range (between 650 and 720 $\mu$s) in 0.1 M TRIS buffer solution (pH = 7.4), while in deuterated water, the luminescence lifetimes vary from 825 to 915 $\mu$s (Table 3, Figure 8b).

The lifetime differences (between 0.1 M aqueous TRIS buffer and deuterated water) can be related to the hydration states of the complexes.[47] Estimates of $q$ reveal no water molecule in the inner sphere for all complexes with bridges longer than that of $[Eu(H(8O2,2)\text{-}1,2\text{-}HOPO)]^-$. Importantly, the obvious luminescence quantum yield differences between $[Eu(H(8O2,2)\text{-}1,2\text{-}HOPO)]^-$ and $[Eu(H(17O5,2)\text{-}1,2\text{-}HOPO)]^-$ are not accompanied by any relevant changes in their luminescence lifetimes. This suggests that while the triplet excited state energies undoubtedly play an important role in the sensitization process differences, the efficiency of the intersystem crossing and the "quantity of energy" accessing the triplet excited state is also a crucial factor that affects the luminescence quantum yield.[48] As explained above, from $[Eu(H(3,2)\text{-}1,2\text{-}HOPO)]^-$ to $[Eu(H(5O,2)\text{-}1,2\text{-}HOPO)]^-$, biexponential decays were obtained (in 0.1 M aqueous TRIS buffer at pH = 7.4 and in deuterated water at room temperature or at 77 K in solid matrix), revealing the presence of two emitting species with ligands having 3−5 atoms in the central bridge. The subsequent measured luminescence lifetimes in deuterated water reveal the presence of two types of complexes, one hydrated and one not. This can be explained by geometric constraints due to the central bridge; the H(2,2) bridge allows only the formation of hydrated complex, while extension of the chain length of the bridge allows better protection of the metal center after complexation by increasing the degrees of freedom between the two terminal $5LIN^{Me}$-1,2-HOPO motifs. This conclusion is supported by the obtained $q$ = 0.3 value for $[Eu(H(3,2)\text{-}1,2\text{-}HOPO)]^-$, which suggests that the propyl chain favors the formation of both an eight- and a nine-coordinate species, since the chain is presumably not long enough to form a single eight-coordinate complex species but is too long to form a single nine-coordinate complex as obtained for $[Eu(H(2,2)\text{-}1,2\text{-}HOPO)]^-$.

Luminescence lifetimes were also determined at 77 K, in a solid matrix (Table 3), which have allowed us to determine whether back energy transfer between the donor triplet excited state and the acceptor manifold excited state of the lanthanide is present or alternately whether quenching via a low-lying LMCT state occurs. In the present case, as can be seen from Table 3, no such quenching can be evidenced since there is only a small difference between the luminescence lifetimes in solution and at low temperature (77 K) in frozen solid solutions.

In terms of their overall luminescence, since the luminescence quantum yield does not take into account the absorptivity of the molecule, a more accurate way to rank the overall efficiency of these compounds is to examine their brightness, typically defined as the product of the luminescence quantum yield with the molar absorption coefficient. For these complexes, as highlighted by the UV−vis absorption study, the molar absorption coefficient decreases by 15% in going from the shorter $[Eu(H(2,2)\text{-}1,2\text{-}HOPO)]^-$ to the longer derivatives (from $[Eu(H(8O2,2)\text{-}1,2\text{-}HOPO)]^-$ to $[Eu(H(17O5,2)\text{-}1,2\text{-}HOPO)]^-$, vide supra). This advantage to the shorter bridge complexes is counterbalanced by the large difference in quantum yield going from 3% to almost 20% for the complexes with longer bridges. This results in an increased brightness by extending the central bridge of these types of chelators going from 655 $M^{-1}\cdot cm^{-1}$ for $[Eu(H(2,2)\text{-}1,2\text{-}HOPO)]^-$ to 2940 $M^{-1}\cdot cm^{-1}$ for $[Eu(H(17O5,2)\text{-}1,2\text{-}HOPO)]^-$, respectively (Figure 6). This latter brightness value is as large as the one obtained for the best bis-tetradentate ligands, typified by $[Eu(5LIN^{Me}\text{-}1,2\text{-}HOPO)_2]^-$ (3400 $M^{-1}\cdot cm^{-1}$).

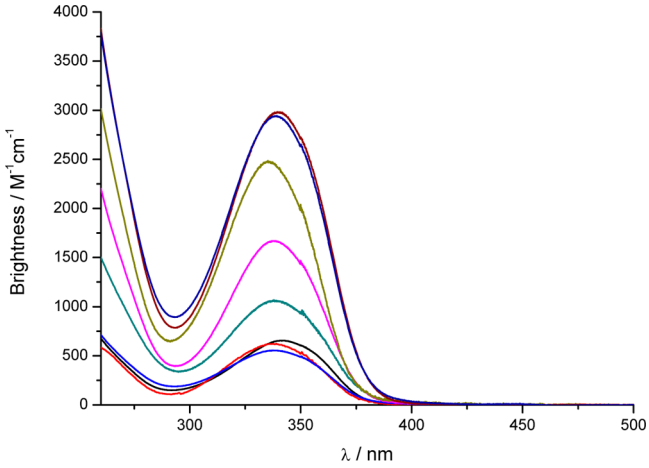


**Figure 6.** Brightness of $[Eu(H(2,2)\text{-}1,2\text{-}HOPO)]^-$ (black), $[Eu(H(3,2)\text{-}1,2\text{-}HOPO)]^-$ (red), $[Eu(H(4,2)\text{-}1,2\text{-}HOPO)]^-$ (blue), $[Eu(H(5O,2)\text{-}1,2\text{-}HOPO)]^-$ (aqua), $[Eu(H(8O2,2)\text{-}1,2\text{-}HOPO)]^-$ (magenta), $[Eu(H(11O3,2)\text{-}1,2\text{-}HOPO)]^-$ (olive), $[Eu(H(14O4,2)\text{-}1,2\text{-}HOPO)]^-$ (blue), and $[Eu(H(17O5,2)\text{-}1,2\text{-}HOPO)]^-$ (dark red) in 0.1 M aqueous TRIS buffer at pH = 7.4.

**Calculated Eu Parameters.** As demonstrated elsewhere,[44,45] the efficiency of the sensitization can be estimated using a method that defines the overall luminescence quantum yield ($\phi_{Eu}$) as the product of the efficiency of the intersystem crossing ($\eta_{ISC}$), the efficiency of the energy transfer ($\eta_{ET}$), and the efficiency of metal-centered luminescence ($\eta_{Eu}$): $\phi_{Eu} = \eta_{ISC}\eta_{ET}\eta_{Eu} = \eta_{sens}\eta_{Eu}$. In this equation, the $\eta_{ISC}\eta_{ET}$ term is termed the sensitization efficiency, $\eta_{sens}$ ($\eta_{sens} = \eta_{ISC}\eta_{ET}$). All luminescence parameters $\tau_R$ (the pure radiative luminescence lifetime) and $k_R$ and $k_{nR}$ (the radiative and nonradiative rate constants) can be deduced from the corrected steady state emission spectrum using a value of $A_{MD,0}$ = 14.65 $s^{-1}$ for the spontaneous emission probability of the $^5D_0 \rightarrow {}^7F_1$ purely magnetic dipole-allowed transition.[49−54] It should be noted


DOI: 10.1021/acs.inorgchem.5b00748
Inorg. Chem. 2015, 54, 6807−6820

**Table 4. Photophysical Data of the Investigated Complexes Containing Only One Species in Aqueous TRIS pH = 7.4 (see Supporting Information for details)**

| | $\phi_{Tot}$ | $\tau$ ($\mu$s) | $\tau_{rad}$ ($\mu$s) | $k_R$ ($s^{-1}$) | $k_{nR}$ ($s^{-1}$) | $\eta_{Eu}$ | $\eta_{sens}$ |
|---|---|---|---|---|---|---|---|
| [Eu(H(2,2)-1,2-HOPO)]$^-$ [29] | 0.036 | 480 | 3000 | 333 | 1750 | 0.160 | 0.225 |
| [Eu(H(8O2,2)-1,2-HOPO)]$^-$ | 0.112 | 697 | 1770 | 566 | 869 | 0.395 | 0.284 |
| [Eu(H(11O3,2)-1,2-HOPO)]$^-$ | 0.165 | 668 | 1630 | 615 | 882 | 0.411 | 0.402 |
| [Eu(H(14O4,2)-1,2-HOPO)]$^-$ | 0.192 | 700 | 1326 | 754 | 674 | 0.528 | 0.364 |
| [Eu(H(17O5,2)-1,2-HOPO)]$^-$ | 0.196 | 704 | 1348 | 742 | 679 | 0.522 | 0.375 |
| [Eu(5LIN$^{Me}$-1,2-HOPO)$_2$]$^-$ [29] | 0.173 | 728 | 1770 | 566 | 807 | 0.412 | 0.420 |

that this approach has its limitations and can lead to large errors, especially when multiple species are present in solution. Hence, these parameters were calculated for five of the octadentate complexes and the model complex which have only one species in solution at pH = 7.4, and the resulting values are reported in Table 4.

As detailed earlier (vide supra), geometric changes around the Eu(III) cation can be seen by integrating the $J = 1$ transition over the entire spectrum, resulting in a decrease of the intensity of $I_{(0,1)}/I_{TOT}$ (Figure 7) for all complexes as a function of the number of atoms in the central bridge.

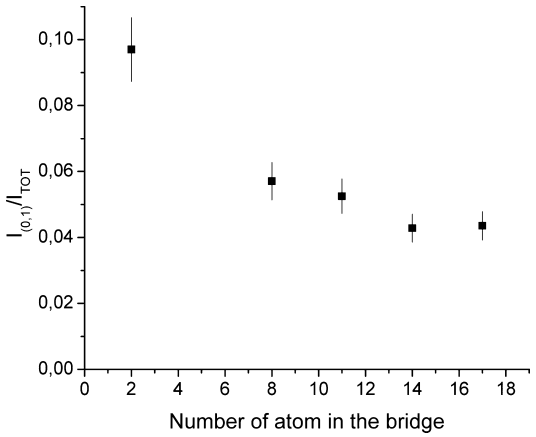


**Figure 7.** Variation of the ratio $I_{(0,1)}/I_{TOT}$ as a function of the number of atoms in the central bridge. Vertical bars represent the error on each point.

As can be readily seen from Table 4, there are some striking similarities among the $k_R$ and $k_{nR}$ values that were also found for the previously reported [Eu(5LIN$^{Me}$-1,2-HOPO)$_2$]$^-$.[46] In detail, the radiative decay rate is smaller than the nonradiative decay for all complexes until [Eu(H(14O4,2)-1,2-HOPO)]$^-$, yielding a metal-centered efficiency inferior to 50%, while for [Eu(H(14O4,2)-1,2-HOPO)]$^-$ and [Eu(H(17O5,2)-1,2-HOPO)]$^-$, the radiative and nonradiative decay are equal, allowing an optimized metal-centered efficiency around 50% to be obtained. This limitation is in line with the results already published for tetradentate 1,2-HOPO derivatives where 50% efficiency seems to be a limit in 0.1 M aqueous TRIS buffer for the 1,2-HOPO derivatives.[9,37,42] Indeed, we note that this increase in the sensitization efficiency by increasing the chain length can partially explain the change of the luminescence quantum yield (Figure 8a), but the observed change can not only be attributed to this phenomenon. The other limitation results from the sensitization process efficiency as illustrated by the value of 28.4% for [Eu(H(8O2,2)-1,2-HOPO)]$^-$ vs 40.2% for [Eu(H(11O3,2)-1,2-HOPO)]$^-$). This result demonstrates that the change in geometry between [Eu(H(8O2,2)-1,2-HOPO)]$^-$ and [Eu(H(11O3,2)-1,2-HOPO)]$^-$ (both complexes being octacoordinated) strongly affects the metal-centered efficiency (as expected) and also influences the sensitization efficiency. This metal-centered efficiency can be further evidenced by looking at the evolution of the radiative lifetimes as a function of the bridge length (Figure 8b).

The values obtained for [Eu(H(11O3,2)-1,2-HOPO)]$^-$ are very close to those obtained for [Eu(5LIN$^{Me}$-1,2-HOPO)$_2$]$^-$ (such as $\eta_{sens}$, $\eta_{Eu}$, $k_{nR}$, quantum yield) and could suggest a similar geometry for these two complexes. While [Eu(H-(14O4,2)-1,2-HOPO)]$^-$ and [Eu(H(17O5,2)-1,2-HOPO)]$^-$

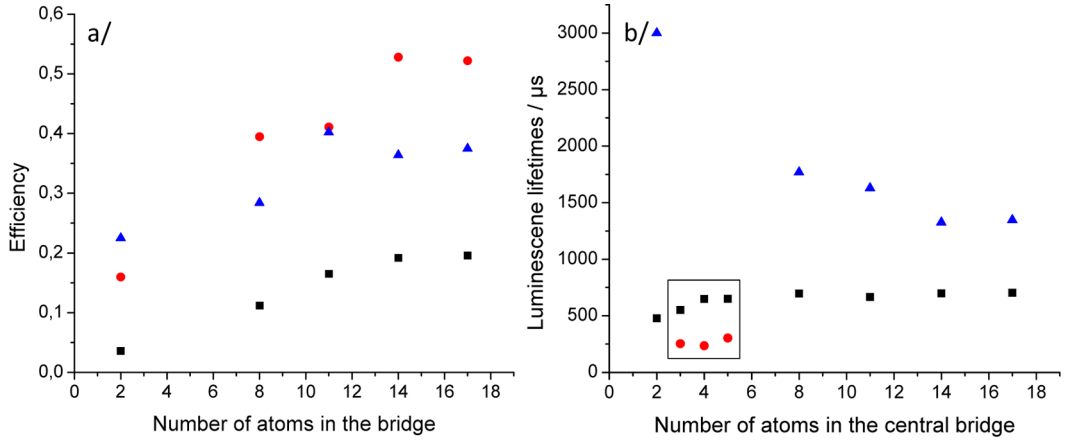


**Figure 8.** (a) Variation of the luminescence quantum yield (■), metal-centered efficiency (●), and sensitization efficiency (▲) as a function of the number of atoms in the central bridge. (b) Variation of the luminescence lifetimes (■) [in the square, (●) second component of the luminescence lifetimes] and radiative luminescence lifetimes (▲) as a function of the number of atoms in the central bridge.



DOI: 10.1021/acs.inorgchem.5b00748
*Inorg. Chem.* 2015, 54, 6807−6820

have a lower ligand-centered sentitization (small $\eta_{sens}$ compared to Eu(H(11O3,2)-1,2-HOPO)]$^-$ and [Eu(5LIN$^{Me}$-1,2-HOPO)$_2$]$^-$), the former two complexes exhibit minimal quenching (large $\eta_{Eu}$, $q$ close to zero, small $k_{nR}$). It is proposed that the longer backbones in these two ligands allow the four 1,2-HOPO to provide optimal shielding of the europium ion from solvent water molecules.

## CONCLUSION

The stability of the reported series of octadentate 1,2-HOPO complexes is higher than the benchmark DTPA, allowing their use at low concentration without any apparent decomplexation.

To obtain optimum brightness, we have shown that all of the steps for the antenna effect have to be optimized; not only the triplet excited state energy drives the sensitization process but also the efficiency of intersystem crossing is important. Other factors such as the symmetry and the geometry of the complex also affect the overall brightness. In the present case, an increase of the central bridge length for octadentate ligands based on the 1,2-HOPO chelator results in improved photophysical properties. This is apparent in the first instance by removing the inner-sphere water molecule present for the [Eu(H(2,2)-1,2-HOPO)$^-$] complex and therefore decreasing the nonradiative decay with longer chains. In the second instance, the increase of the luminescence properties can also be attributed to a change in the geometry around the metal center. This yields some interesting luminescence properties for [Eu(H(14O4,2)-1,2-HOPO)]$^-$ and [Eu(H(17O5,2)-1,2-HOPO)]$^-$ which also have high thermodynamic stabilities in aqueous solution at pH = 7.4. These properties are significantly improved when compared to the model compound [Eu(5LIN$^{Me}$-1,2-HOPO)$_2$]$^-$, resulting in optimized luminescence properties for an octadentate structure containing the 1,2-HOPO moiety, with a brightness that is large enough to yield complexes which may be of considerable use for in vitro and in cellulo biological measurements.

## ASSOCIATED CONTENT

### Supporting Information

The Supporting Information contains HRESI mass spectral data, plots of luminescence dependence at different pH and Ca(II) concentrations, Zn(II) competition batch titrations and luminescence decay fits for the Eu(III) complexes. The Supporting Information is available free of charge on the ACS Publications website at DOI: 10.1021/acs.inorgchem.5b00748.

## AUTHOR INFORMATION

### Corresponding Author

*Phone: 510-642-7219. Fax: 510-642-5324. E-mail: raymond@socrates.berkeley.edu.

### Notes

The authors declare the following competing financial interest(s): Some of this technology is licensed to Lumiphore, Inc. in which some of the authors have a financial interest.

## ACKNOWLEDGMENTS

Early portions of this work were partially supported by the NIH (Grant HL69832) and then subsequently supported by the Director, Office of Science, Office of Basic Energy Sciences, and the Division of Chemical Sciences, Geosciences, and Biosciences of the U.S. Department of Energy at LBNL under Contract No. DE-AC02-05CH11231. The authors thank Prof. Gilles Muller (San Jose State University) for the use of a low-temperature time-resolved luminescence spectrometer. L.J.D. is grateful for a postdoctoral fellowship of the Alexander von Humboldt Foundation.

## REFERENCES

(1) Herman, B.; Tanke, H. J. *Fluorescence Microscopy*; Garland Science: United Kingdom, 1997.
(2) Mason, W. T. *Fluorescent and luminescent probes for biological activity: a practical guide to technology for quantitative real time analysis*; SPIE Publications: Cambridge, UK, 1999.
(3) Zwier, J. M.; Bazin, H.; Lamarque, L.; Mathis, G. *Inorg. Chem.* **2014**, *53*, 1854−1866.
(4) J. C. G. Bünzli and Choppin, G. R. *Lanthanide probes in life, chemical and earth sciences: Theory and practice*; Elsevier: Amsterdam, 1989.
(5) Bünzli, J. C. G. *Chem. Lett.* **2009**, *38*, 104−109.
(6) Bünzli, J. C. G. *Chem. Rev* **2010**, *110*, 2729−2755.
(7) Bünzli, J.-C. G.; Eliseeva, S. V. *Chem. Sci.* **2013**, *4*, 1939−1949.
(8) Latva, M.; Takalob, H.; Mukkala, V.-M.; Matachescuc, C.; Rodriguez-Ubisd, J. C.; Kankarea, J. *J. Lumin.* **1997**, *75*, 149−169.
(9) D'Aléo, A.; Xu, J.; Moore, E. G.; Jocher, C. J.; Raymond, K. N. *Inorg. Chem.* **2008**, *47*, 6109−6111.
(10) Walton, J. W.; Bourdolle, A.; Butler, S. J.; Soulie, M.; Delbianco, M.; McMahon, B. K.; Pal, R.; Puschmann, H.; Zwier, J. M.; Lamarque, L.; Maury, O.; Andraud, C.; Parker, D. *Chem. Commun. (Cambridge, U.K.)* **2013**, *49*, 1600−1602.
(11) Matsuya, T.; Hoshino, N.; Okuyama, T. *Curr. Anal. Chem.* **2006**, *2*, 397−410.
(12) Pintacuda, G.; John, M.; Su, X.-C.; Otting, G. *Acc. Chem. Res.* **2007**, *40*, 206−212.
(13) John, M.; Schmitz, C.; Park, A. Y.; Dixon, N. E.; Huber, T.; Otting, G. *J. Am. Chem. Soc.* **2007**, *129*, 13749−13757.
(14) Harris, K. L.; Lim, S.; Franklin, S. J. *Inorg. Chem.* **2006**, *45*, 10002−10012.
(15) Yang, K.; Wang, L.; Wu, J.; Dong, F. *J. Inorg. Biochem.* **1993**, *52*, 145−150.
(16) Kostova, I.; Traykova, M.; Rastogi, V. K. *Med. Chem.* **2008**, *4*, 371−378.
(17) Yuan, J.; Wang, G. *Trends Anal. Chem.* **2006**, *25*, 490−500.
(18) Hemmila, I. *J. Biomol. Screen.* **1999**, *4*, 303−307.
(19) Hemmila, I. A. *Immunochemistry* **1997**, 193−214.
(20) Allicotti, G.; Borras, E.; Pinilla, C. J. *Immunoassay Immunochem.* **2003**, *24*, 345−358.
(21) Moore, E. G.; Samuel, A. P. S.; Raymond, K. N. *Acc. Chem. Res.* **2009**, *42*, 542−552.
(22) Butler, S. J.; Lamarque, L.; Pal, R.; Parker, D. *Chem. Sci.* **2014**, *5*, 1750−1756.
(23) Bourdolle, A.; Allali, M.; Mulatier, J.-C.; Le Guennic, B.; Zwier, J. M.; Baldeck, P. L.; Bünzli, J.-C. G.; Andraud, C.; Lamarque, L.; Maury, O. *Inorg. Chem.* **2011**, *50*, 4987−4999.
(24) Daumann, L. J.; Tatum, D. S.; Snyder, B. E. R.; Ni, C.; Law, G.-l.; Solomon, E. I.; Raymond, K. N. *J. Am. Chem. Soc.* **2015**, *137*, 2816−2819.
(25) Sturzbecher-Hoehne, M.; Kullgren, B.; Jarvis, E. E.; An, D. D.; Abergel, R. J. *Chem.−Eur. J.* **2014**, *20*, 9962−9968.
(26) Liu, M.; Wang, J.; Wu, X.; Wang, E.; Abergel, R. J.; Shuh, D. K.; Raymond, K. N.; Liu, P. *J. Pharm. Biomed. Anal.* **2015**, *102*, 443−449.
(27) Deri, M. A.; Ponnala, S.; Zeglis, B. M.; Pohl, G.; Dannenberg, J. J.; Lewis, J. S.; Francesconi, L. C. *J. Med. Chem.* **2014**, *57*, 4849−4860.
(28) Durbin, P. W.; Kullgren, B.; Xu, J.; Raymond, K. N. *Radiat. Prot. Dosim.* **1998**, *79*, 433−443.
(29) Moore, E. G.; Jocher, C. J.; Xu, J.; Werner, E. J.; Raymond, K. N. *Inorg. Chem.* **2007**, *46*, 5468−5470.
(30) Eaton, D. F. *Pure Appl. Chem.* **1988**, *60*, 1107−1114.
(31) Doble, D. M. J.; Melchior, M.; O'Sullivan, B.; Siering, C.; Xu, J.; Pierre, V. C.; Raymond, K. N. *Inorg. Chem.* **2003**, *42*, 4930−4937.


DOI: 10.1021/acs.inorgchem.5b00748
*Inorg. Chem.* 2015, 54, 6807−6820

(32) Pierre, V. C.; Botta, M.; Aime, S.; Raymond, K. N. *Inorg. Chem.* **2006**, *45*, 8355−8364.
(33) de Bettencourt-Dias, A.; Barber, P. S.; Bauer, S. *J. Am. Chem. Soc.* **2012**, *134*, 6987−6994.
(34) Samuel, A. P. S.; Moore, E. G.; Melchior, M.; Xu, J. D.; Raymond, K. N. *Inorg. Chem.* **2008**, *47*, 7535−7544.
(35) Bernhardt, P. V. *Inorg. Chem.* **2001**, *40*, 1086−1092.
(36) Xu, J.; Churchill, D. G.; Botta, M.; Raymond, K. N. *Inorg. Chem.* **2004**, *43*, 5492−5494.
(37) Moore, E. G.; Xu, J.; Jocher, C. J.; Werner, E. J.; Raymond, K. N. *J. Am. Chem. Soc.* **2006**, *128*, 10648−10649.
(38) Sherry, A. D.; Caravan, P.; Lenkinski, R. E. *J. Magn. Reson. Imaging* **2009**, *30*, 1240−1248.
(39) Mathis, G. *J. Biomol. Screening* **1999**, *4*, 309−313.
(40) Smith, A. E.; Martell, R. M. *Critical Stability Constants*; Plenium Press: New York, 1974.
(41) Raymond, K.; Xu, J. N. In *The Development of Iron Chelators for Clinical Use*; Bergeron, R. J., Brittenham, G. M., Eds.; CRC Press: Boca Raton, FL, 1994.
(42) Moore, E. G.; Xu, J.; Jocher, C. J.; Castro-Rodriguez, I.; Raymond, K. N. *Inorg. Chem.* **2008**, *47*, 3105−3118.
(43) Moore, E. G.; Xu, J.; Jocher, C. J.; Werner, E. J.; Raymond, K. N. *J. Am. Chem. Soc.* **2006**, *128*, 10648−10649.
(44) Beeby, A.; Bushby, L. M.; Maffeo, D.; Williams, J. A. G. *J. Chem. Soc., Dalton Trans.* **2002**, 48−54.
(45) Werts, M. H. V.; Jukes, R. T. F.; Verhoeven, J. W. *Phys. Chem. Chem. Phys.* **2002**, *4*, 1542−1548.
(46) Moore, E. G.; Jocher, C. J.; Xu, J.; Werner, E. J.; Raymond, K. N. *Inorg. Chem.* **2007**, *46*, 5468−5470.
(47) Supkowski, R. M.; Horrocks, W. D. *Inorg. Chimi. Acta* **2002**, *340*, 44−48.
(48) D'Aléo, A.; Picot, A.; Beeby, A.; Williams, J. A. G.; Le Guennic, B.; Andraud, C.; Maury, O. *Inorg. Chem.* **2008**, *47*, 10258−10268.
(49) Werts, M. H. V.; Jukes, R. T. F.; Verhoeven, J. W. *Phys. Chem. Chem. Phys.* **2002**, *4*, 1542−1548.
(50) Hehlen, M. P.; Brik, M. G.; Krämer, K. W. *J. Lumin.* **2013**, *136*, 221−239.
(51) Judd, B. R. *Phys. Rev.* **1962**, *127*, 750−761.
(52) Ofelt, G. S. *J. Chem. Phys.* **1962**, *37*, 511−520.
(53) Kirby, A. F.; Richardson, F. S. *J. Phys. Chem.* **1983**, *87*, 2544−2556.
(54) Görller-Walrand, C.; Binnemans, K. *Handb. Phys. Chem. Rare Earths* **1998**, 101−264.


DOI: 10.1021/acs.inorgchem.5b00748
*Inorg. Chem.* 2015, 54, 6807−6820